



Cite this: *Nanoscale*, 2025, **17**, 22733

## Smart wearable fibers and textiles: status and prospects

Weiye Zhang,<sup>†a</sup> Shuo Luan,<sup>†a</sup> Mingwei Tian,<sup>a</sup> Lijun Qu,<sup>a</sup> <sup>a</sup> Xueji Zhang,<sup>b</sup> Tingting Fan<sup>\*a</sup> and Jinlei Miao <sup>\*a,c</sup>

As an emerging revolutionary technology, smart wearables can be directly worn on the body; integrated into clothes; and exhibit desirable characteristics, including light weight, portability, softness and natural conformity to the curved human body surface. Because of the high air permeability, compatibility with the human body, and wear comfort of textiles, the seamless integration of the smart wearable technology with textiles is regarded as the future direction for essential development. The use of fiber electronics as building units to weave smart wearable textiles can not only endow traditional clothes with multiple intelligent functions and wearable systems with ideal breathability, but can also provide endurance to modern textile processing technologies such as knitting and weaving, which opens up a brand-new path for the large-scale application of wearable electronics. This review comprehensively summarizes the state-of-the-art advancements in smart wearable fibers and textiles, including smart materials, properties, fabrication strategies, surface modifications, and smart wearable applications. We focus on advanced smart wearable fibers and textiles, which could simultaneously exhibit excellent multi-functions and highly comfortable wearable experience even under large mechanical deformations, and discuss the strategies and mechanisms that are suitable for fabricating smart wearable fibers and textiles with excellent signal capture and transmission reliability. Finally, a critical discussion of the opportunities and challenges associated with smart wearable fibers and textiles towards practical wearable applications is presented.

Received 2nd July 2025,  
Accepted 7th September 2025

DOI: 10.1039/d5nr02801a

[rsc.li/nanoscale](http://rsc.li/nanoscale)

### 1. Introduction

Clothes play a crucial role in our daily lives, which not only provide us with basic thermal comfort but also protect the human body from the surrounding environmental harms such as insect or mosquito bites and extreme weather impacts.<sup>1–3</sup> With the continuous development of science and technology, textiles are no longer limited to traditional cold protection and warm insulation functions. Fibers and textiles weave through the entire development process of human civilization and the long evolution history of human science technology.<sup>4,5</sup> Nowadays, modern clothing has been endowed with more unique functions, making it much more suitable for specific fields, for example, functional clothing such as medical protec-

tive clothing, fire-resistant clothing, and space clothing.<sup>6</sup> In recent years, there has been a widespread consensus that fabrics should play a key role as the second skin of the human body. Fabrics should function similarly as the sensing skin layer of the human body, rather than simply providing warmth and insulation function.<sup>7</sup> As an important medium for the interaction between the human body and the surrounding environment, fabrics play a crucial role in energy and material exchange between the human body and the environment. However, for a relatively long period of time, research on the advanced multiple functions of fabrics such as temperature regulation, healthcare management, and human-machine interactions has gained insufficient attention.

Integrating electronic devices into textiles is considered an ideal approach to obtain advanced multi-functional fabrics.<sup>8–10</sup> Unfortunately, traditional electronic devices are usually relatively heavy, rigid, bulky, and brittle, making it difficult to seamlessly integrate them with soft fibers and fabrics. In this regard, flexible and stretchable electronics exhibit outstanding characteristics such as softness, lightness, resistance to mechanical deformations, and integration into complex curved surfaces, overcoming the limitations of traditional electronic devices such as rigidity, heaviness, and brittleness.<sup>11</sup> They are widely used in fields such as flexible

<sup>a</sup>Shandong Key Laboratory of Medical and Health Textile Materials, State Key Laboratory of Bio-Fibers and Eco-Textiles, Research Center for Intelligent and Wearable Technology, College of Textiles & Clothing, Qingdao University, Qingdao 266071, P. R. China. E-mail: [tingtingfan@qdu.edu.cn](mailto:tingtingfan@qdu.edu.cn), [jinlei.miao@qdu.edu.cn](mailto:jinlei.miao@qdu.edu.cn)

<sup>b</sup>School of Biomedical Engineering, Shenzhen University Health Science Center, Shenzhen, Guangdong 518060, P. R. China

<sup>c</sup>Textile Ecological Dyeing and Finishing Key Laboratory of Sichuan Province, Chengdu Textile College, Chengdu, Sichuan 610097, P. R. China

<sup>†</sup>These authors contribute equally to this work

sensors, foldable displays, electronic skins (E-skins), bending-resistant perovskite solar cells/light-emitting diodes, stretchable circuits, and soft robots, which have received significant attention.<sup>12–14</sup> Especially, with the comprehensive entry of humanity into the era of artificial intelligence (AI), flexible electronics have become more and more important. As the foundation of the Internet of Things (IoT), flexible and stretchable electronics can attach to the curved joint surface of the human body, collect real-time physiological and health data, and transmit it to the big data cloud computing platform terminal.<sup>15</sup> Hospitals and medical personnel can remotely monitor the health status of the human body in real time, quickly analyze and evaluate it, and take timely and effective health care and emergency rescue measures. Flexible and stretchable electronics, as a key path to improve the efficiency of medical and health services and precise individual health management, such as modern medical monitoring devices that fit the human body, such as Apple iWatch and Huawei wristbands, can effectively monitor a series of health conditions (e.g. sweat, blood sugar, blood pressure, sleep depth, pulse, heart rate, muscle signals) in real time, which have very broad application prospects and important research values.<sup>16,17</sup> Hence, in recent years, to simultaneously realize comfortable wearable applications and intelligent functions, smart wearable fibers and textiles integrated with flexible and stretchable electronics have been developed and deeply investigated.

Smart wearable fibers and textiles are a novel type of sensing devices that can perceive environmental conditions such as force, heat, moisture, and other physical stimuli, and can respond while retaining textile properties and styles.<sup>18</sup> The development of smart materials has laid the foundation for the development of smart fibers and smart textiles, promoting the development of advanced fabrics. Smart fiber is a type of fiber that integrates sensing and information processing, obtained by processing smart materials onto the fiber. At present, smart fiber materials are mainly divided into two categories: one category comprises textile materials that have sensing functions for external or internal stimuli (such as stress, strain, light, electricity, magnetism, heat, moisture, chemistry, biology, and electromagnetic radiation), called “sensing materials”, which can be used to make various textile-based flexible sensors, and another type comprises materials that can respond or drive changes in the external environment or internal state, and can be used to make various drivers (actuators).<sup>19,20</sup> Currently, smart fibers that have been mass-produced include fiber sensors, joule-heating fibers, photothermal fibers, temperature regulating fibers, color changing fibers, and energy harvesting/storage fibers. For example, Zuo *et al.*<sup>3</sup> developed an intelligent multi-responsive aramid aerogel fiber that utilizes light/electricity/thermal conversion to achieve personal thermal management and energy conversion/storage. Cai *et al.*<sup>18</sup> fabricated a gel-based composite material with a broad working range (2800%), fast response capability (90 ms), and excellent repeatability, making it suitable for human motion monitoring. Similarly, Wang *et al.*<sup>21</sup> designed an MXene textile-based elastic core-

spun yarn sensor capable of dual strain/humidity sensing, which can be applied in monitoring human motion and physiological signals. While challenges still remain, particularly for complex multifunctional intelligent systems and seamless integration, these emerging smart wearable fibers and textiles represent significant development directions in academia and industry fields.

In this review, the state-of-the-art advancements in emerging smart wearable fibers and textiles are summarized (Scheme 1). First, the intelligent materials and properties of high-performance smart wearable fibers and textiles provide a solid foundation for their versatility and application potential. These materials not only possess high sensitivity, flexibility and conductivity, but also could maintain stable performance under complex environmental conditions. Second, this review discusses in detail the manufacturing technologies of smart fibers and textiles, including electrostatic spinning, coating method, and composite fiber/textile fabrication. These technological advances have made the large-scale production of smart wearable fibers and textiles possible. In addition, this paper analyzes a wide range of applications of smart wearable fibers and textiles in various fields including health monitoring, human-computer interaction, thermal management, electromagnetic shielding, energy harvesting and storage. Although great challenges such as wearable comfort, breathability, ergonomic compatibility, abrasion resistance, stretchability, and washability still remain, these challenges are expected to be solved through interdisciplinary collaboration and technological innovation. Future research will focus more on developing environmentally friendly and sustainable solutions to fully realize the potential of smart wearable fibers and textiles to drive changes in industries such as healthcare and sports technology. Finally, a critical discussion of the opportunities and challenges of smart wearable fibers and textiles towards practical wearable applications is also presented.

## 2. Smart materials and properties

Smart materials are advanced materials that can perceive and respond to external environmental changes such as temperature, pressure, and humidity. They are widely used in fields such as smart textiles, flexible electronic devices, and health monitoring. These materials achieve multifunctionality, high sensitivity, and good flexibility by integrating nanotechnology, materials science, and electronic engineering, providing strong support for wearable technology and personalized medicine. This review summarizes the commonly used smart materials and properties in the field of smart wearable fibers and textiles (Table 1).

### 2.1 Carbon-based nanomaterials

Carbon-based nanomaterials mainly include carbon black, carbon nanotubes (CNTs), carbon nanofibers (CNFs), graphene, graphene oxide (GO), and reduced graphene oxide (rGO).<sup>22</sup> Due to their excellent conductivity ( $\sim 10^4$  S cm<sup>-1</sup>),



**Scheme 1** Smart wearable fibers and textiles: status and prospects. Reproduced from ref. 46 with permission from American Association for the Advancement of Science, copyright 2024. Reproduced from ref. 50 with permission from Elsevier, copyright 2023. Reproduced from ref. 62 with permission from John Wiley and Sons, copyright 2025. Reproduced from ref. 57 with permission from American Chemical Society, copyright 2021. Reproduced from ref. 86 with permission from American Chemical Society, copyright 2019. Reproduced from ref. 102 with permission from John Wiley and Sons, copyright 2024. Reproduced from ref. 114 with permission from John Wiley and Sons, copyright 2022. Reproduced from ref. 118 with permission from Royal Society of Chemistry, copyright 2022.

thermal conductivity, chemical stability, and mechanical properties, they have received widespread attention in recent years.<sup>21,23</sup> Among them, one-dimensional (1D) CNTs and 2D graphene nanosheets have shown great potential in flexible and stretchable electronics and smart wearable textile products.<sup>24</sup>

**2.1.1 Graphene.** Graphene is a 2D lamellar carbon nanomaterial<sup>25</sup> with a very stable structure and extremely high mechanical strength, with a Young's modulus of up to 1 TPa and a tensile strength of 130 GPa, making it one of the strongest materials known to date, while graphene also exhibits excellent mechanical flexibility and can be bent.<sup>11</sup> Graphene exhibits excellent electrical properties due to its low resistivity ( $\sim 10^{-6} \Omega \text{ cm}$ ) and high carrier mobility ( $15\,000 \text{ cm}^2 \text{ V}^{-1} \text{ s}^{-1}$ ).<sup>26</sup> In addition, graphene has outstanding thermal conductivity, and the thermal conductivity of pure graphene nanosheet could reach as high as  $5300 \text{ W m}^{-1} \text{ K}^{-1}$ , which is much higher than that of CNTs and is the highest thermal conductivity among existing carbon materials.<sup>27</sup> Graphene has become an ideal material for building smart fabrics due to its excellent mechanical strength, electrical conductivity, thermal conductivity and environmental stability.<sup>28</sup> Currently, the main prepa-

ration methods of graphene include mechanical exfoliation, liquid-phase exfoliation, chemical vapor deposition, epitaxial growth and redox methods.<sup>25–27</sup>

Graphene is strongly chemically inert, which makes it difficult to be effectively dispersed in solvents for large-scale solution processing. Chen *et al.*<sup>26</sup> prepared graphene-based conductive fibers by using MXene nanosheets as dispersants for graphene, and assembling AgNWs core-interlocked graphene sheaths along elastic polyurethane (PU) fibers with a core-sheath dual network (Fig. 1a). The conductive fibers exhibit reliable response (response speed of 440 ms) to various stimuli (*e.g.* mechanical, electrical, thermal, and optical) under large mechanical deformations and can seamlessly adapt to human body movements, converting mechanical deformations into physiological signals for accurate healthcare monitoring. It also has excellent Joule heat and photothermal effects, exhibits immediate thermal energy harvesting/storage during stimulus response, and shows dynamic camouflage performance when integrated with phase change and thermochromic layers, which is promising for personalized healthcare and thermal management. The strong chemical inertness of graphene nanosheets makes them difficult to be effectively dis-

**Table 1** Comparison of nanomaterials for smart wearable fibers and textiles

Nanomaterials	Advantage	Disadvantage	Applications
Graphene	<ul style="list-style-type: none"> <li>Highly conductive</li> <li>High mechanical strength</li> </ul>	<ul style="list-style-type: none"> <li>High cost of making single-layer graphene</li> <li>Graphene flakes are easily stacked and poorly dispersed</li> <li>Fiber integration is difficult</li> </ul>	<ul style="list-style-type: none"> <li>Flexible sensors</li> <li>Lightweight supercapacitors</li> </ul>
CNTs	<ul style="list-style-type: none"> <li>High thermal conductivity</li> <li>Good chemical stability</li> <li>Highly conductive</li> <li>High mechanical strength</li> <li>High thermal conductivity</li> <li>Good chemical stability</li> <li>Easy fiber consolidation</li> </ul>	<ul style="list-style-type: none"> <li>High cost of preparation of single-walled carbon nanotubes</li> <li>Easy to agglomerate and poorly dispersed</li> </ul>	<ul style="list-style-type: none"> <li>Thermoregulatory fabrics</li> <li>Electrothermal fibers/fabrics</li> <li>High-sensitivity strain sensors</li> <li>Woven into smart fabric circuits</li> <li>Military/medical protective suits</li> <li>Thermal management</li> </ul>
AgNWs	<ul style="list-style-type: none"> <li>Highly conductive</li> <li>Good flexibility</li> <li>Easy fiber consolidation</li> </ul>	<ul style="list-style-type: none"> <li>High cost</li> <li>Poor chemical stability</li> <li>Weak mechanical properties</li> </ul>	<ul style="list-style-type: none"> <li>Transparent conductive fabrics</li> <li>Flexible sensors</li> <li>Electromagnetic shielding</li> <li>Electrothermal fibers/fabrics</li> <li>Thermal management</li> <li>Friction nanogenerators</li> </ul>
LM	<ul style="list-style-type: none"> <li>High conductivity</li> <li>High-thermal conductivity</li> <li>High strength</li> <li>Mobility</li> </ul>	<ul style="list-style-type: none"> <li>High surface tension</li> <li>High cost</li> <li>Easy to oxidize</li> <li>Easy to leak</li> </ul>	<ul style="list-style-type: none"> <li>Electronic skin</li> <li>Stretchable electronic devices</li> <li>Flexible electronic devices</li> <li>Software robots</li> </ul>
Conductive polymers	<ul style="list-style-type: none"> <li>Low cost</li> <li>Easy fiber consolidation</li> </ul>	<ul style="list-style-type: none"> <li>Poor conductivity</li> <li>Poor mechanical properties</li> <li>Poor environmental stability (easily oxidized)</li> </ul>	<ul style="list-style-type: none"> <li>Stretchable electrodes</li> <li>Transparent heating films</li> <li>Flexible sensors</li> </ul>
MXene	<ul style="list-style-type: none"> <li>Good electrical conductivity</li> <li>Low cost</li> <li>Easy fiber consolidation</li> </ul>	<ul style="list-style-type: none"> <li>General mechanical properties</li> <li>General environmental stability</li> <li>Less conductive than graphene and carbon nanotubes</li> </ul>	<ul style="list-style-type: none"> <li>Thermal management</li> <li>Friction nanogenerators</li> <li>EMI shielding textiles</li> <li>Flexible supercapacitors</li> <li>Pressure sensors</li> </ul>

persed in solvents for large-scale solution processing. Liang's team<sup>29</sup> prepared hydrophilic graphene conductive materials by using natural silk gum in order to overcome the defects of graphene, which is difficult to be dispersed without hydrophilicity and prone to agglomeration. The flexible E-textile prepared using the hydrophilic graphene conductive material not only has the characteristics of high breathability and water washing resistance, but also can be used as a flexible sensor to monitor complex human activities and convert the resulting mechanical signals into electrical signals, which successfully realizes human motion detection and health monitoring, and it is an important research direction in the field of smart wearable technology (Fig. 1b).

GO is the oxidation product of graphene nanosheet, which still maintains the layered structure of graphite. Compared with graphene, GO has an increased number of oxygen-containing functional groups, and hence, it is more active in nature and has superior hydrophilicity. GO can be well dispersed in water, and is more widely noticed because of its low production cost and ease of processing. Tang's team<sup>30</sup> controlled the assembly behavior of GO precursor by optimizing its surface chemistry and used wet spinning to prepare a GO precursor with high strength, high toughness, and highly conductive graphene fibers with a tensile strength of 791.7 MPa, a toughness of 8.3 MJ m<sup>-3</sup>, and an electrical conductivity of 1.06 × 10<sup>5</sup> S m<sup>-1</sup>. This work provides a simple, efficient, and scalable method for the preparation of high-performance, multi-functional graphene fibers and flexible fibrous wearable electronic devices (Fig. 1c–e).

**2.1.2 Carbon nanotubes.** Carbon nanotubes (CNTs) are 1D tubular carbon-based nanomaterials formed by curling layers of graphene sheets. Depending on the number of layers in the tube wall, they are classified as single-walled carbon nanotubes (SWCNTs) and multi-walled carbon nanotubes (MWCNTs). CNTs have a large aspect ratio >1000, a high specific surface area of 50–1315 m<sup>2</sup> g<sup>-1</sup>, extremely high strength and toughness (Young's modulus of 1–5 TPa), excellent electrical properties and chemical stability, which are widely used in wearable devices.<sup>31,32</sup>

Hu's team<sup>33</sup> prepared a multifunctional carbon nanotube-based aerogel film by doping carbon nanotubes into ANFs and hydrophobically modifying it with fluorocarbon resin (Fig. 1f). The prepared multifunctional aerogel film has excellent hydrophobicity (WCA = 137.0°), a large specific surface area (232.8 m<sup>2</sup> g<sup>-1</sup>), and good flexibility, while exhibiting a high electrical conductivity (230 S m<sup>-1</sup>), realizing a good Joule thermal effect and electromagnetic shielding performance, which has been widely investigated by researchers in the field of smart wearable, personal thermal management and electromagnetic shielding. Gao *et al.*<sup>34</sup> fabricated ultra-high stretchable conductive CNTs and polyurethane (PU) nanofiber spiral yarns by a simple electrostatic spinning, coating and twisting process (Fig. 1g–i). The yarn achieves stable conductivity and recovery over a deformation range of 900% and maintains conductivity even after stretching to 1700%. This ultra-highly stretchable, low-cost CNTs/PU spiral yarn shows strong competitiveness in smart wearable textiles, large strain sensors, soft robots, and smart actuators. Jiang *et al.*<sup>35</sup> prepared a core/shell



**Fig. 1** (a) Schematic of core sheath heterogeneous interlocked conductive fiber-enabled smart textile for personalized healthcare and thermal management. Reproduced from ref. 26 with permission from John Wiley and Sons, copyright 2023. (b) Characterization of hexamethylene diisocyanate-crosslinked silk gel-graphene (HSG) textiles and schematic representation of an integrated multi-sensing system based on HSG textiles. Reproduced from ref. 29 with permission from John Wiley and Sons, copyright 2022. (c) Schematic illustration of the preparation processes of f-GO, f-GO fiber, and reduced f-GO fiber. (d) Tensile stress strain curves of f-GO fibers fabricated with different nozzles. (e) Comparison of the tensile strength and toughness of f-GO fibers fabricated with different nozzles. Reproduced from ref. 30 with permission from John Wiley and Sons, copyright 2022. (f) Temperature evolution of the FC-ANF/CNT aerogel films under stepwise-increased/decreased power inputs. The IR images in the inset demonstrate the nonwetting state of the film under 4 V. Reproduced from ref. 33 with permission from American Chemical Society, copyright 2020. (g) Good conductivity of the helical CNTs/PU yarn demonstrated by liquid crystal display (LED) light during the stretching process. (h) Helical yarn with uncoiling during the stretching process. (i) FEA calculation of the helical yarn stretch process, theoretically explaining the correlation between the structure and elongation. Reproduced from ref. 34 with permission from American Chemical Society, copyright 2020.

stretchable conductive fiber composite by dip-coating CNTs onto poly(m-phenylene isophthalamide) fibers (FWNT/PMIA) and annealing it by a post-heating process. The composite fiber exhibits high electrical conductivity and signal transmission stability, and the conductivity decreases by only  $13 \text{ S cm}^{-1}$  during the stretching process, and this stable electrical conductivity in stretchable fibers is very important for the wearable application in stretchable electronic products.

Although graphene and CNTs have attracted much attention due to their excellent properties, their high fabrication cost makes large-scale preparation still a challenge, while their nonpolar structure leads to poor dispersion in common sol-

vents. In addition, the large aspect ratio and strong van der Waals forces of graphene and CNTs make them prone to agglomeration and difficult to disperse. The development of suitable solvents for the preparation of graphene and CNTs, the realization of large-scale production, and the achievement of their good dispersion are still challenges that need to be solved in the future.

## 2.2 Metallic materials

Metallic materials have a wide range of applications in the wearable field due to their excellent electrical and thermal conductivity, mechanical properties and chemical stability. For

the metallic material-based smart wearable applications, which could range from electromagnetic shielding to flexible sensors, and from electrothermal elements to energy storage, metallic materials provide an important material basis for the rapid development of smart wearable technologies and systems.<sup>36,37</sup>

**2.2.1 Silver nanowires.** Metallic nanomaterials are an important class of nanomaterials, which show high mechanical flexibility and effectively avoid the rigidity characteristic of traditional macroscopic metal materials. Metallic nanomaterials, which have an extremely wide range of applications in flexible wearable fiber electronics because they fully combine the high electrical and thermal conductivities of

metallic materials with the unique properties of nanomaterials, mainly including 0D materials and 1D materials.<sup>38</sup> One-dimensional metallic nanomaterials have a diameter of less than 100 nm and a large aspect ratio, such as 1D silver nanowires (AgNWs) with a high electrical conductivity of  $6.3 \times 10^7 \text{ S m}^{-1}$ , thermal conductivity and chemical stability, which have been widely used in the wearable electronics.<sup>39,40</sup>

Fan *et al.*<sup>41</sup> prepared a flexible leaf vein template using NaOH etching of leaves, and a transparent conductive mesh was biomimetic prepared by assembling AgNWs intertwined with MXenes in the etching grooves in an orderly manner along the fibers (Fig. 2a). The sheet resistance can be as low as  $0.5 \Omega \text{ sq}^{-1}$  with a quality factor (FoM) of 3523 when the trans-



**Fig. 2** (a) Schematic of the fabrication of wearable electrodes. (b) Picture of bending wearable electrodes. Reproduced from ref. 41 with permission from American Chemical Society, copyright 2022. (c) Schematics of LMEA with Fe incorporated liquid metal droplets as phase transition inclusion. The temperature rise caused by stretching (200% strain) (d) and twisting (e) during LMEA solidification is displayed. Reproduced from ref. 46 with permission from American Association for the Advancement of Science, copyright 2024. (f) Schematic of the corresponding synergistic effect between 1D CNTs and 2D graphene. (g) Optical photos of intelligent fibers under different mechanical deformations. Reproduced from ref. 50 with permission from Elsevier, copyright 2023. (h) Voltage of a 22  $\mu\text{F}$  capacitor charged by the WP-TENG at different motion frequencies in 2 min. (i) Voltage of a 22  $\mu\text{F}$  capacitor charged by the WP-TENG with hand patting. (j) Rectified current output of the WP-TENG at different motion frequencies. Reproduced from ref. 51 with permission from John Wiley and Sons, copyright 2018.

mittance of the fibrous electrode is 81.6%, and the resistance of the fibrous electrode remains almost unchanged during 2000 bending cycles. The transparent conductive network has great potential in high-performance wearable optoelectronics and camouflage electronics. Han's team<sup>42</sup> prepared a multi-functional thermally conductive composite film based on AgNWs by using BNNS-ANFs as the matrix and AgNWs as the reinforcing functional body. The chemical decomposition and *in situ* growth methods were used to provide the composite film with excellent electrical and thermal conductivity (thermal conductivity of  $9.44 \text{ W m}^{-1} \text{ K}^{-1}$ ), excellent fracture strength of 136 MPa, and flexible, sensitive, and stable strain, electrothermal, and photothermal sensing properties, which will play an important role in the field of communication materials and smart sensors. Ma *et al.*<sup>43</sup> reported the use of flower-shaped silver nanoparticles with nanodisc-shaped petals (Ag nanoflowers) and polyurethane synthesized by a scalable wet-spinning process for highly conductive stretchable fibers. The fiber exhibited a very high electrical conductivity of  $41\,245 \text{ S cm}^{-1}$ , a high Young's modulus of 731.5 MPa and an ultimate strength of 39.6 MPa. The fibers exhibited elasticity after pre-stretching and the change in resistance of the weft fabric is negligible at 200% strain. Smart fibers with very high electrical conductivity, tensile properties and mechanical strength can be used for wearable electronics applications.

**2.2.2 Liquid metals.** Liquid metals (LMs) are metals that are liquid at room temperature or higher, also known as low-melting-point metals. LMs have high electrical conductivity, mobility, nano-manipulability and excellent surface properties. It can be precisely manipulated by electric and magnetic fields and can be deformed under the influence of gravity. LMs can combine with polymers to form highly conductive networks suitable for flexible circuit boards. Its oxide film promotes adhesion on different substrates and performs well in biocompatibility, such as gallium-based liquid metals with low toxicity and good biocompatibility *in vivo*, which can be widely used in wearable and implantable devices.<sup>44</sup>

Jiang *et al.*<sup>45</sup> proposed a solvent-assisted dispersion (SAD) method, which utilizes the fragmentation and reintegration of LMs in volatile solvents to engulf and disperse the filler, and successfully integrated MXenes into LM homogeneously. The prepared MXene/LM (MLM) coatings exhibit high electromagnetic interference (EMI) shielding performance (105 dB at  $20 \mu\text{m}$ ). In addition, the rheological properties of the MLM coatings make them ductile and facilitate direct printing and adaptation to various structures. This study provides an efficient convenient way to assemble LMs from low-dimensional materials and paves the way for the development of multifunctional soft devices. Wang *et al.*<sup>46</sup> prepared a smart soft architecture by incorporating magnetized liquid metal droplets into a highly stretchable elastomer network. The supercooled liquid metal droplets act as microscopic latent heat reservoirs whose controlled solidification releases local heat energy/information flow for programmable visualization and display. The elastomer can be sensed by thermal and/or thermochromic

imaging for various information-encoded contact (mechanical pressing, stretching, and torsion) and non-contact (magnetic field) stimuli, as well as for the visualization of dynamic phase transitions and stress evolution processes. The LM elastomer architecture provides a versatile platform for designing soft smart sensing, display and information encryption systems (Fig. 2c–e).

Although metal materials have many advantages, some metal nanomaterials are poorly biocompatible and prone to skin inflammation, while metal nanomaterials may be oxidized and have poor stability in long-term use. LMs have high surface tension and poor adhesion to the substrate, while there is also a risk of leakage due to the fluidity of liquid metals. Currently, researchers are mostly working on solving the stability of metal nanomaterials and overcoming the surface tension of liquid metals.

### 2.3 Conductive polymers

Conductive polymers are polymer materials with conjugated electronic systems in the carbon skeleton materials. Conductive polymers are simple to prepare, have good conductivity, good electrochemical advantages and mechanical properties. It not only has its intrinsic conductivity, but also can be doped with other materials to achieve a unique conductive function with much higher conductivity. The conductive polymers have alternating single and double bonds along the polymer chain, creating a system of delocalized pi-electrons, which is the foundation for conductivity. They are usually insulators or semiconductors in their pristine (undoped) state. Conductivity can be achieved through chemical or electrochemical doping, which either removes electrons (p-doping) or adds electrons (n-doping) to the backbone, creating charge carriers (polarons and bipolarons). Conductive polymer fibers are organic conductive fibers derived by direct spinning of conductive polymers, and composite conductive fibers can also be prepared by wet spinning, melting, and mixing methods. Conductive polymers not only have the flexibility of plastics, but also exhibit the conductivity of certain low-conducting metals, which play an increasingly important role in wearable electronics.<sup>47–49</sup> The well-studied inherently conductive polymers (ICPs) include polyacetylene (PA), polyaniline (PANI), polythiophene (PT), and polypyrrole (PPy).<sup>48</sup>

He *et al.*<sup>50</sup> developed a super-stretchable multi-responsive phase-change smart fiber by encapsulating phase-change material (PCM) microcapsules in elastic polyurethane (PU) *via* wet-spinning and bonding inorganic CNTs/graphene along the surface of the elastic fibers *via* interfacial bonding of poly(3,4-ethylenedioxythiophene):polystyrene sulfonate (PEDOT:PSS) (Fig. 2f and g). The smart fiber has a high electrical conductivity of  $1.96 \times 10^4 \text{ S m}^{-1}$  and exhibits high sensitivity to multiple stimuli (mechanical/electrical/thermal/photo-optical), as well as a high mechanical stretchability >200%, which allows it to seamlessly adapt to drastic and large displacements, and good Joule heating and photo-thermal effects even under large mechanical deformations. The flexible PCM-based stretchable multi-responsive fibers have great potential in emerging wear-

able electronics and smart textiles. Wen *et al.*<sup>51</sup> fabricated a transparent and stretchable friction nanogenerator (WP-TEG) based on PEDOT:PSS electrodes, and the developed wearable WP-TEG exhibited good stretchability and transparency with a maximum tensile strain of  $\approx 100\%$ . In addition, by attaching to the curved human skin, the WP-TEG can be used as an active human motion monitoring sensor, which can detect the bending angle of the human elbow and joints by analyzing the peaks of the voltage output and monitor the frequency of the motion by counting the peaks. The excellent energy harvesting and active sensing capabilities of the WP-TEG, as well as its superior transparency and stretchability, show its potential for use in the fields of human-machine interaction, electronic skin, soft robotics, wearable electronics, and other novel promising wearable applications (Fig. 2h–j). Zhu *et al.*<sup>52</sup> developed a novel fibrous hydrogen ( $H_2$ ) sensor by directly electrochemically depositing a long palladium (Pd) sensing layer on a conductive PEDOT:PSS fiber electrode. This method produces self-supporting functional fibers (PEDOT:PSS@Pd). It has flexibility, light weight, braiding ability, and high mechanical strength. The response times of the PEDOT:PSS@Pd fiber optic sensor at 1% and 4%  $H_2$  are 34 ( $\pm 6$ ) s and 19 ( $\pm 4$ ) s, respectively, demonstrating excellent sensing performance. In addition, the fiber optic sensors maintain good sensing performance under different mechanical bending states, demonstrating the great potential for constructing wearable sensor devices to detect hydrogen gas leaks in a timely manner. This work provides an intelligent design strategy for fiber optic gas sensors, which has certain development potential in the field of wearable electronic products.

Although conductive polymers such as ICPs are easy to integrate with fibers and have good processability, they are poorly conductive compared with inorganic materials such as graphene, CNTs, and AgNWs. Their mechanical properties are not high, and they often need to be composited with other materials to improve their mechanical stability, and at the same time, conductive polymers are poorly environmentally stable and prone to oxidation, which have severely hindered the development of conductive polymers.

#### 2.4 MXenes

MXene is an inorganic compound composed of transition metal nitrides and carbides with a 2D lamellar structure, which can be obtained by selectively etching the MAX phase of 3D lamellar compounds with strong acids or bases.<sup>53–55</sup> MXenes contain a large number of oxygen-containing functional groups, which can interact with other materials to form a chemical bond, thus improving the mechanical and electrical properties of other materials, and at the same time, MXenes also exhibit amphiphilicity, excellent electrical and thermal conductivity, and high mechanical strength (Young's modulus of 330 GPa and tensile strength of 344 MPa).<sup>56–58</sup> MXenes have attracted much attention in the field of wearable fibers/textiles due to their unique properties.

Hou *et al.*<sup>59</sup> prepared an adhesive mussel-inspired polydopamine-functionalized MXene (PDM) as an interfacial solder

and assembled AgNWs onto highly elastic fibers to form stretchable conductive fibers with a core–sheath heterogeneous interlocking structure, which not only exhibited excellent electrical conductivity ( $1.13 \times 10^5 \text{ S m}^{-1}$ ), but also could be stable under large mechanical deformation (300%) (Fig. 3a and b). This super-stretchable fiber conductor is promising in the field of soft electronics. Zheng *et al.*<sup>60</sup> prepared MXene fibers with high flexibility and electrochemical properties through interfacial crosslinking and oriented structure (Fig. 3c–e). The fiber has a high electrical conductivity of  $3545 \text{ S cm}^{-1}$ , a high mechanical strength of 205.5 MPa, and a high pseudo-capacitive charge storage capacity of  $1570.5 \text{ F cm}^{-3}$ . The assembled MXene-based fiber capacitors could maintain 99.5% capacitance under mechanical deformation and can be integrated into textiles to power wearable electronic devices. This work provides a new avenue for the fabrication of advanced MXene-based smart fibers and the development of high-performance flexible fiber supercapacitors. Cheng *et al.*<sup>61</sup> prepared a stretchable piezoresistive sensor by spraying MXene nanosheets onto PDMS using a shorthand printing process, which has a high sensitivity of  $151.4 \text{ kPa}^{-1}$ , a fast response time  $< 130 \text{ ms}$  and an ultra-low pressure monitoring limit of 4.4 Pa, which can withstand more than 10 000 tensile cycles. In addition, its randomly distributed microstructure is similar to that of human skin, which can be used for human signal monitoring and quantitative monitoring of pressure distribution (Fig. 3f–h). He *et al.*<sup>62</sup> developed high-performance MXene-based lightweight conductive fibers with extremely high electrical conductivity and mechanical flexibility by double-scale spatial confinement spinning. *Via* wet-spinning, MXene nanosheets were oriented to achieve directional assembly, and at the same time, the ordered extension of carbon nanofibers was adjusted, so that the assembled MXene nanosheets could be assembled in an orderly manner, and the carbon nanofibers were extended in an orderly manner. The assembled MXene fibers with an excellent high mechanical strength of 506.7 MPa and an electrical conductivity of  $1.27 \times 10^6 \text{ S m}^{-1}$  pave the way for the ordered assembly of nanosheets for use in next-generation smart wearable fibers and textiles (Fig. 3i–k).

Although MXenes, emerging 2D materials, have attracted widespread attention in the field of smart wearable fibers/fabrics due to their unique properties, their stability in the environment is poor. Achieving their large-scale preparation, improving their environmental stability, and maintaining their long-term stable conductivity and other properties remain great challenges.

Smart materials have been widely applied in smart textiles, flexible electronic devices, health monitoring, and other fields in recent years due to their unique properties. Among these, carbon-based nanomaterials (graphene, carbon nanotubes) exhibit high electrical/thermal conductivity, large specific surface area, and high mechanical strength. However, due to their non-polar structure, they tend to agglomerate and are difficult to disperse in ordinary solvents, and they are prone to oxidation and cracking in humid and hot environments. Metal

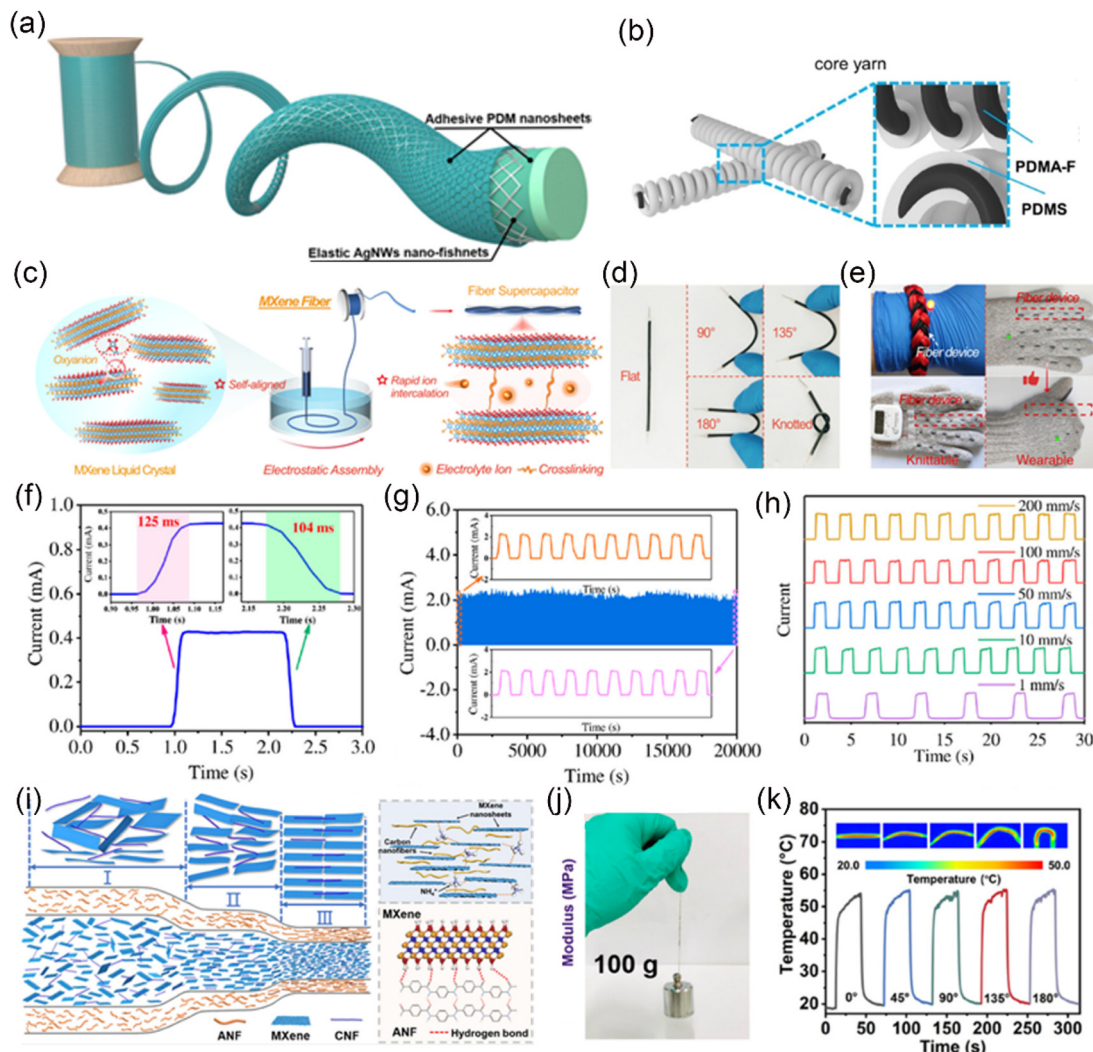


**Fig. 3** (a) Schematic of MXene-based smart fibers. (b) Schematic of the wearable sensor based on PDMA-F conductors. Reproduced from ref. 59 with permission from American Chemical Society, copyright 2025. (c) Fabrication of MXene fibers and their assembled fiber supercapacitors. (d) Photographs of the fiber supercapacitor with different mechanical deformations, including flat, under bending angles of 90°, 135°, and 180° and knotted state. (e) Photographs of fiber supercapacitors embedded in a hand-knitted wristband to power a red LED and integrated into the commercial glove to power an electronic watch, and photographs of fully charged fiber supercapacitors integrated into the glove to illuminate a green LED under mechanical deformation. Reproduced from ref. 60 with permission from American Chemical Society, copyright 2023. (f) I T curve indicates the responsive and recovery time of the sensor under 0.73 kPa. (g) Excellent cycle stability performance of the device after 10 000 pressure cycling tests under 3.36 kPa. (h) Piezoresistive sensors exhibit superior sensing performance uniformity at different speeds under 2.1 kPa. Reproduced from ref. 61 with permission from American Chemical Society, copyright 2020. (i) Schematic of the gradual alignment of 2D MXenes and 1D CNFs with different dimensions and shapes during the dual-spatially confined wet-spinning process. (j) MXene-CNF@ANF coaxial fibers can support a weight of 100 g. (k) Temperature time curves of single MXene-CNF@ANF fibers at bending angles from 0° to 180°. Reproduced from ref. 62 with permission from John Wiley and Sons, copyright 2025.

materials have been studied for their high electrical and thermal conductivity. Silver nanowires, in particular, exhibit high aspect ratios and stretchability, but they have poor chemical stability and are prone to oxidation, leading to a significant increase in resistance. Liquid metals possess self-healing and oxidation-resistant properties, but they can corrode other metals and pose a risk of leakage. Conductive polymers have good processability and are easy to combine with fibers, but they have low conductivity and are prone to oxidation. MXenes' unique amphiphilic properties make them easy to integrate with fibers,

but they have poor environmental stability and are prone to oxidation when exposed to air for extended periods, leading to a decrease in conductivity. In summary, conductive polymers are cost-effective and easy to integrate, but their conductivity is lower than that of other nanomaterials. If conductivity is a priority, high-conductivity carbon-based nanomaterials, metallic materials, and MXenes can be selected. However, when making actual choices, both the conductivity of nanomaterials and production costs should be comprehensively considered to achieve a balance between the two.

### 3. Fabrication techniques

The manufacturing strategies of smart wearable fibers/textiles are pivotal in balancing intelligent functionality, wearable comfort, and scalability. Based on the integration mechanisms of conductive/functional building blocks with textile substrates, current techniques can be categorized into two paradigms: surface engineering and fiber-level hybridization. Each approach exhibits unique advantages in achieving wearability-performance equilibrium (Fig. 4).

#### 3.1 Surface engineering strategies

Intelligent functional materials are deposited on the surface of fibers/textiles using physical or chemical methods to build conductive or responsive networks, enabling rapid prototyping and low-cost production. The commonly used primary surface modification-based fabrication strategies include immersion, spraying, screen printing, magnetron sputtering, *in situ* synthesis, and related methodologies.

Compared to conductive materials with inferior dispersibility, such as graphene and CNTs, MXenes form a more homo-

geneous conductive network. Fan *et al.*<sup>63</sup> incorporated silver nanoparticles (AgNPs) and MXenes as conductive fillers into a polymer matrix, subsequently coating the composite onto waterborne polyurethane (WPU) (Fig. 4a). Utilizing the plasma effect of AgNPs and the high photothermal conversion efficiency of MXenes, the fabricated E-skin exhibits excellent photothermal performance and thermal conductivity, achieving a temperature rise of 111 °C in 5 minutes under 600 mW cm<sup>-2</sup> light irradiation, while maintaining a transmittance of 83% at a thickness of 60 μm. This coating, enabling spatially controlled heating and rapid self-healing, provides a novel strategy for developing robotic E-skins. Although dip-coating offers advantages such as process simplicity, high production efficiency, and low cost, its application is constrained by poor interfacial adhesion between conductive materials and substrates, leading to delamination under mechanical deformation.

Spray coating is a facile and efficient methodology that employs high-pressure airbrush systems to deposit atomized droplets onto substrate surfaces, thereby constructing interconnected point-to-point conductive networks. This technique has gained extensive application in intelligent wearable elec-



**Fig. 4** (a) Schematic of AgNPs@MXene-PU coating preparation and illumination. Reproduced from ref. 63 with permission from American Chemical Society, copyright 2019. (b) Schematic of MXene and AgNW coating-modified nonwovens and sensing characterization. Reproduced from ref. 57 with permission from American Chemical Society, copyright 2021. (c) Schematic of the manufacture of a Ni/NiO double-layer temperature sensor. Reproduced from ref. 64 with permission from Elsevier, copyright 2021. (d) Textile sensors whose resistivity is closely adjusted by the dense weft. Reproduced from ref. 65 with permission from American Chemical Society, copyright 2022. (e) Aqueous MXene/xanthan gum hybrid ink. Reproduced from ref. 66 with permission from John Wiley and Sons, copyright 2022. (f) MXene/rGO/ANF composite aerogels prepared by freeze-drying and thermal reduction. Reproduced from ref. 67 with permission from Elsevier, copyright 2022.

tronics due to its operational simplicity, rapid processing capability, and compatibility with flexible substrates. Liu *et al.*<sup>57</sup> fabricated a multifunctional stimulus-responsive textile by depositing MXene nanosheets and AgNWs onto a nonwoven substrate *via* a spray-coating strategy (Fig. 4b). This engineered textile exhibits exceptional photothermal and electrothermal conversion capabilities, coupled with highly sensitive and stable strain-sensing performance (gauge factor (GF) = 1085) and remarkable breathability. The synergistic effect arising from the interconnected conductive network—where 1D AgNWs bridge 2D MXene nanosheets—endows the fabric with superior electrical conductivity  $\sim 5.8 \text{ S cm}^{-1}$  and mechanical durability, maintaining functionality over 1500 repetitive stretching cycles. Such hierarchical architecture demonstrates significant potential for applications in personalized health-care monitoring and adaptive thermal management systems.

Magnetron sputtering is a physical vapor deposition (PVD) technique that is achieved by bombarding a solid cathode (target) with electrified gas ions in a vacuum environment. This process moves atoms away from the target surface through momentum transfer and subsequently condenses onto the substrate to form a thin film with controlled stoichiometry. It is the main method for manufacturing thin films in microelectronics and optical coatings. Appiagyei *et al.*<sup>64</sup> prepared a flexible Ni/NiO bilayer temperature sensor without patterning on a cylindrical PET fiber substrate using a radio frequency magnetron sputtering technology (Fig. 4c). The temperature coefficient of resistance (TCR) reached  $3.8 \times 10^{-3} \text{ }^\circ\text{C}^{-1}$  (linearity  $R^2 = 0.9852$ ), significantly higher than that of single-layer Ni ( $3.2 \times 10^{-3} \text{ }^\circ\text{C}^{-1}$ ) or NiO ( $3.1 \times 10^{-3} \text{ }^\circ\text{C}^{-1}$ ). After 16 000 bending cycles (curvature radius 20 mm), the TCR remained stable at  $1.0 \times 10^{-4} \text{ }^\circ\text{C}^{-1}$ . The sensor also exhibited stable sensing performance in acidic/alkaline solutions (pH 1–13), tap water, and detergent-containing environments. This work demonstrated the high efficiency and reliability of magnetron sputtering in fabricating highly flexible and environmentally corrosion-resistant temperature sensing elements.

*In situ* synthesis is a materials engineering strategy that enables the direct growth of functional particles within a substrate matrix through controlled chemical reactions. This technique yields uniformly dispersed nanostructures with intrinsic advantages of particle–substrate interfacial integrity and environmental benignancy, making it particularly suitable for constructing conductive networks and fabricating flexible wearable electronics. Li *et al.*<sup>65</sup> achieved *in situ* growth of polyaniline with P(NIPAM-AA) adhesives to fabricate wearable textile sensors. Surface resistivity and volume resistivity are regulated by the density of the weft and warp (Fig. 4d). The surface resistance decreases rapidly under tensile force, while the vertical resistance decays exponentially under pressure, with resistance change  $\Delta R < 90\%$  at 20 N. It is used as an induction finger sleeve and a smart insole, and exhibits a fast response (delay < 0.1 seconds). The smart wearable textile does not require an electrode pattern and can be used directly for human activity monitoring.

Screen printing enables rapid fabrication of conductive patterns on flexible substrates *via* mesh-template deposition.

Wu *et al.*<sup>66</sup> developed an aqueous MXene/xanthan gum hybrid ink, exhibiting tunable rheological properties and long-term stability, facilitating high-resolution screen printing of densely stacked flexible (Fig. 4e) films with electrical conductivities reaching  $4.8 \times 10^4 \text{ S m}^{-1}$  significantly exceeding values reported for prior MXene composites. This ink enables the fabrication of multifunctional devices: electromagnetic interference shielding components demonstrate an average shielding effectiveness of 54.2 dB in the X-band (8.2–12.4 GHz) with >98% efficiency retention after 1000 bending cycles. Joule heating elements achieve rapid thermal ramp rates of  $20 \text{ }^\circ\text{C s}^{-1}$  and maximum steady-state temperatures of  $130.8 \text{ }^\circ\text{C}$  under a 4 V driving voltage, and the interdigitated piezoresistive sensors exhibit a response time of 130 ms under applied pressures up to 30 kPa. The eco-friendly aqueous formulation and compatibility with diverse flexible substrates (PET, paper, and PI) underscore its potential for scalable integration within next-generation wearable electronics and systems.

### 3.2 Fiber-level hybridization techniques

Intelligent functional materials are embedded within fiber matrices during spinning processes to achieve intrinsic conductivity, responsiveness, and mechanical robustness, enabling seamless integration with textile manufacturing. Compared to fiber surface treatments, the integral forming method achieves significantly stronger interfacial bonding between conductive materials and fiber matrices, resulting in more robust conductive networks. Primary fabrication strategies include blended spinning, direct cross-linking of nanomaterials, and hierarchical structural compositing.

Blending spinning is a widely utilized technique in which conductive materials are uniformly dispersed within a spinning precursor solution, followed by fabrication through various fiber spinning processes. Xie *et al.*<sup>67</sup> successfully fabricated a ternary MXene/rGO/ANFs composite aerogel *via* freeze-drying followed by thermal reduction (Fig. 4f). Within this structure, ANFs serve as a mechanically reinforcing skeleton, while rGO and MXene synergistically construct a conductive network. This approach leverages hydrogen bonding at the interface between functional groups on the ANF surface and MXene/rGO. The resulting aerogel exhibits a compressive strength of 200 kPa at 70% strain with an ultralow density of merely  $0.062 \text{ g cm}^{-3}$ , coupled with excellent compression resilience (recovering its original state after 100 compression cycles). Furthermore, it demonstrates outstanding electromagnetic interference (EMI) shielding performance, achieving an efficiency of 54.8 dB in the X-band. This work paves the way for the design of lightweight, high-strength, and highly efficient EMI shielding wearable devices. Recent advances have seen the development of a flexible wearable hydrogel system<sup>68</sup> that incorporates a GO-enhanced NC matrix with a wide strain detection range (>300%) and high sensitivity (gauge coefficient of 3.04) and fast autonomous self-healing capability (stress self-healing efficiency up to 85%) (Fig. 5a). Wang *et al.*<sup>69</sup> innovatively fabricated GNPs/ANF composite fibers *via* a wet-spin-



**Fig. 5** (a) Schematic of the preparation of GO-enhanced wearable hydrogels and self-healing verification and sensing test diagrams. Reproduced from ref. 68 with permission from American Chemical Society, copyright 2024. (b) Schematic of the preparation of GNP/ANF composite fibers by wet spinning technology. Reproduced from ref. 69 with permission from Elsevier, copyright 2021. (c) Oriented sheet-assembled graphene fibers and their microstructures. Reproduced from ref. 70 with permission from Springer Nature, copyright 2011. (d) Schematic of the preparation of high-performance CNT fibers. Reproduced from ref. 71 with permission from Springer Nature, copyright 2022. (e) Schematic of the preparation of PEDOT:PSS fibers with high conductivity in wet spinning. Reproduced from ref. 72 with permission from Royal Society of Chemistry, copyright 2019. (f) Schematic of coaxial spinning fibers with high conductivity stability. Reproduced from ref. 73 with permission from American Association for the Advancement of Science, copyright 2021.

ning technique, leveraging the electrostatic repulsion and interfacial interactions (*e.g.*  $\pi$ - $\pi$  stacking) of ANFs to overcome the challenges of high-concentration dispersion and spinnability of low-oxidized GNPs (Fig. 5b). The branched network structure of ANFs effectively suppressed GNP aggregation through electrostatic repulsion and non-covalent interactions. The resulting fibers simultaneously achieved ultrahigh electrical conductivity ( $4236 \text{ S m}^{-1}$ ), exceptional tensile strength (227.5 MPa), and fracture elongation (10.2%). Remarkably, the fibers maintained stable conductivity after 5000 bending cycles. This work provides a novel wire solution integrating high-efficiency

conduction, mechanical robustness, and processability for wearable electronics.

The conductive network constructed *via* the blending-spinning method is discretely distributed within the fiber matrix, demonstrating exceptional structural stability under external stimuli and frictional stresses. However, the intrinsically electrically insulating nature of the polymeric fiber matrix imposes a fundamental limitation on conductivity, typically resulting in composite fibers with compromised electrical conductivity (generally exhibiting resistivity  $>10^2 \text{ } \Omega \text{ cm}$ ) despite their mechanical robustness.

Conductive nanomaterials can be crosslinked without polymer additives to form continuous fibers directly. Recent advances in nanomaterial research have enabled the development of conductive fibers such as PEDOT:PSS fibers, CNTs fibers, graphene fibers, and MXene-based fibers. Notably, the absence of insulating polymers endows these fibers with exceptional electrical and thermal conductivity. However, since the fiber strength relies solely on interfacial interactions between low-dimensional nanomaterials, their longitudinal flexibility still requires further enhancement. Xu *et al.*<sup>70</sup> innovatively leveraged the self-assembly characteristics of graphene chiral liquid crystals to achieve a helically ordered arrangement of graphene nanosheets *via* a controllable shear flow field (Fig. 5c). These aligned structures were subsequently processed into macroscopic graphene fibers using wet-spinning technology. The resulting fibers exhibit both ultrahigh electrical conductivity ( $>10^4$  S m<sup>-1</sup>) and exceptional mechanical strength ( $>500$  MPa), thereby pioneering the application of 2D nano-conductive materials in flexible wearable devices. Liu *et al.*<sup>71</sup> developed a continuous process that directly converts waste lignin into high-performance CNT fibers (Fig. 5d). The resulting fibers achieve an electrical conductivity of  $1.19 \times 10^4$  S m<sup>-1</sup> and a tensile strength of 1.33 GPa while exhibiting excellent flexibility. This technology addresses the long-standing challenge of low CNT crystallinity and significantly advances the development of green electronic materials. Zhang *et al.*<sup>72</sup> prepared highly conductive PEDOT:PSS fibers by wet-spinning (Fig. 5e). By using concentrated sulfuric acid (H<sub>2</sub>SO<sub>4</sub>) coagulation baths, they quickly and efficiently remove PSS in a matter of seconds during fiber formation. The resulting fibers exhibit a highly arranged structure, excellent mechanical strength (tensile strength of 435 MPa) and ultra-high electrical conductivity (3828 S cm<sup>-1</sup>). These fibers can be further used to develop flexible wearable sensors and supercapacitors with fast response times (20 ms) and high sensitivity. Conductive fibers fabricated *via* direct nanomaterial forming methods exhibit excellent electrical properties. Conversely, due to the stringent requirements and high costs associated with conductive materials, scalable production of pure conductive nanomaterial-based smart fibers remains a challenge. Furthermore, their relative low mechanical strength limits standalone applications.

Hierarchical structural synthesis refers to a specialized technique that integrates a functional material with a fiber matrix by means of a unique structure (*e.g.* coaxial or multi-layer membrane structures and then twist into fibers) without changing the intrinsic composition of the fiber. The former can be achieved by wet or electrostatic spinning, while the latter relies mainly on electrostatic spinning.

Zheng *et al.*<sup>73</sup> developed core–sheath fibers with a liquid metal (eutectic gallium–indium, EGaIn) core *via* coaxial spinning technology (Fig. 5f). The high fluidity and percolation characteristics of the LM conductive network effectively compensate for channel defects induced by fiber stretching, yielding fibers with exceptional electrical conductivity ( $4.35 \times 10^4$  S m<sup>-1</sup>) and mechanical stretchability (1170%). The fibers' resis-

tance variation (4%) is even under 200% strain, demonstrating remarkable stability. He *et al.*<sup>62</sup> employed a coaxial wet-spinning technology to encapsulate MXenes and cellulose nanofibers (CNFs) with polymer nanofibers, ANFs, innovatively proposing a dual spatially confined spinning strategy (Fig. 6a). The resulting fibers exhibited exceptional mechanical properties (506.7 MPa) and high electrical conductivity ( $1.27 \times 10^6$  S m<sup>-1</sup>), along with remarkable flexibility and weavability. Based on this advancement, the researchers constructed a highly sensitive capacitive sensor capable of monitoring physiological signals such as pulse rate (67 bpm) and vocal vibrations, demonstrating significant potential in wearable health monitoring applications.

Electrostatic spinning is a spinning method in which a polymer solution is extruded and dispersed under a high-voltage electrostatic field into micron- or nanometer-sized fibers, which are subsequently deposited and formed on a grounded collector. Electrostatic spinning is simple to operate, the fiber architecture is controllable, and the processing cost is low. Inter-fiber void channels can be formed during the fabrication process, and so electrospun membranes exhibit easy modification, breathability and water resistance. Electrostatically spun membranes are commonly used in smart textile sensors and wearable E-skins.

Wu *et al.*<sup>74</sup> developed a thermoregulatory flexible fibrous membrane (EPU@PW) based on a hierarchical core–sheath fiber structure using coaxial electrospinning technology (Fig. 6b). In this membrane, polyurethane (PU) serves as the sheath layer to encapsulate the PCM, paraffin wax (PW, melting point 20–38 °C). The surface was sequentially modified with CNTs, polydopamine (PDA), and the conductive polymer PEDOT:PSS, forming a multifunctional hierarchical structure. This design integrates three functions: phase change energy storage, photothermal conversion, and Joule heating. Cao *et al.*<sup>75</sup> fabricated a conductive metallic film through the *in situ* assembly of electrospun thermoplastic polyurethane (TPU) nanofiber scaffolds with electrospayed eutectic gallium–indium (EGaIn) liquid metal nanoparticles (Fig. 6c). This composite film exhibits a minimal resistance variation of only 350% under a substantial tensile strain of 570%. Furthermore, it demonstrates exceptional cycling stability, maintaining its electrical properties (with only a 5% increase in resistance) after 330 000 stretching cycles at 100% strain. The material also possesses outstanding environmental resistance, including tolerance to acids/alkalis, high temperatures, and water immersion. These properties make it promising for applications in medical detection and electronic skin.

Continuous advancements in novel fabrication methods are optimizing the performance of fibers and textiles. However, there are still significant challenges in the compatibility of advanced functionalization technologies with traditional industrial production. The inherent low throughput ( $\leq 0.5$  m min<sup>-1</sup>) and fragile nanofibers of electrospinning prove catastrophic when subjected to high-speed weaving tension or needle penetration, causing irreparable structural damage. Similarly, *in situ* synthesis techniques rely on batch-soaking



**Fig. 6** (a) Schematic and flexible display of coaxial wet-spun MXene-CNF@ANF fibers. Reproduced from ref. 62 with permission from John Wiley and Sons, copyright 2025. (b) Schematic of the preparation of coaxial electrospun multilayer structure fiber membranes. Reproduced from ref. 74 with permission from American Chemical Society, copyright 2022. (c) Electrostatic spraying of liquid metal particle-modified electrospun TPU fiber films and the high elasticity of its surface microstructure agent. Reproduced from ref. 75 with permission from John Wiley and Sons, copyright 2022. (d) Schematic of a fabric of conductive yarn (cellulose yarn treated with PEDOT:PSS) and metal electrodes (aluminum wire). Reproduced from ref. 76 with permission from John Wiley and Sons, copyright 2023. (e) Double-needle bed weft knitting process interweaves conductive weft yarns (ionized gel fibers) and luminescent warp yarns (ZnS fluorescent coated fibers) into smart fabrics. Reproduced from ref. 77 with permission from Springer Nature, copyright 2021.

processes involving toxic solvents that can disrupt the continuous production line and introduce harmful contaminants into water-based textile processing environments. While spraying allows for moderate production speeds ( $5\text{--}20\text{ m min}^{-1}$ ), its effectiveness is affected by constant nozzle clogging and shading effects that can create uneven conductivity in complex weave textures or knitted loop structures. Wet spinning can produce conductive yarns directly, but incur significant solvent recovery costs while being less compatible with natural fiber substrates. Crucially, these challenges become more pronounced during the standard textile finishing stage, where the mechanical softening process wears down nanoscale conductive pathways. This systemic conflict between precision functionalization and high-volume manufacturing leads to reduced performance and higher costs during scale-up. Moreover, significant challenges remain for their practical and commercial deployment due to the constraints of real-world production conditions. Mass production faces hurdles related to cost efficiency and yield, while the processes for specialized

fabrication techniques still require refinement. Furthermore, the integration of conventional textile processing technologies with the production of smart fibers and textiles presents additional challenges that need to be resolved.

## 4. Structure design

To achieve smart wearable fibers and textiles, superior conductive materials and advanced manufacturing processes are indispensable. The fiber matrix serves as both a carrier and channels for conductive materials while withstanding and mitigating deformation induced by external stimuli. Concurrently, conductive materials are required to establish continuous pathways and networked architectures capable of perceiving and responding to mechanical deformations of the fiber substrate. Consequently, initial developments in flexible smart products predominantly focused on PDMS and other biocompatible materials with favorable flexibility and stability.

However, most of these polymer-based systems are synthesized through direct reactions into film-like structures exhibiting poor breathability, which renders them prone to cause skin irritation when employed in wearable applications, significantly compromising wear comfort. This limitation has driven emerging interest in fiber-based architectures with inherent comfort characteristics for smart electronics. Additionally, textiles featuring elastic properties and hierarchically breathable structures demonstrate unique advantages in the development of flexible wearable electronic devices, particularly through their synergistic integration of mechanical compliance and functional sensing capabilities.

The functional performance of smart wearable textiles is inherently controlled not only by advanced smart materials, but also by their structure. As a physical scaffold that interfaces with the human body and carries functional components, the fabric structure determines key attributes such as mechanical suitability, signal transduction efficiency, and wearing comfort. Textile-based devices utilize intrinsic structural features, such as the elasticity of knitted loops, the matrix regularity of woven meshes, or the porous network of non-woven fabrics, to achieve seamless integration with dynamic human movements. This section systematically examines the three main structural paradigms (woven, knitted and nonwoven) to enable flexible wearables.

#### 4.1 Woven fabrics

Woven fabrics are characterized by a regular and stable geometric configuration formed through the perpendicular interlacing of warp and weft yarns. This inherent orthogonal structure not only endows woven fabrics with exceptional dimensional stability and anisotropic mechanical properties but also establishes them as an ideal platform for the precise integration of functional conductive elements, such as MXenes, AgNWs, CNTs, and graphene. Through precision weaving techniques—including variations in fundamental weaves (*e.g.*, plain, twill, satin) and the implementation of multi-layer structures—it becomes possible to exert precise control over the distribution density, orientation, and contact points of conductive yarns. This controlled integration facilitates the targeted modulation of diverse functionalities. Consequently, woven fabrics represent one of the predominant structural formats in current research and application within the field of smart textiles.

Deng *et al.*<sup>76</sup> developed a self-powered smart textile incorporating a dynamic Schottky diode (DSD) matrix through weaving processes that interlace conductive yarns (PEDOT:PSS-treated cellulose yarns) with metallic electrodes (aluminum wires) (Fig. 6d). This architecture enables biaxial motion detection capabilities: warp-directional pressure activates normal-direction sensing (sensitivity:  $0.12 \text{ kPa}^{-1}$ ), while weft-directional sliding facilitates tangential motion perception. The study demonstrated that the woven structure not only streamlines sensor network integration (“weaving-as-manufacturing”) but also overcomes the limitations of conventional single-point sensing *via* signal amplification and distributed detec-

tion mechanisms. Shi *et al.*<sup>77</sup> employed a double needle-bed weft knitting process to integrate conductive weft yarns (ionic gel fiber) and light-emitting warp yarns (ZnS phosphor-coated fibers) (Fig. 6e). At their contact points, electroluminescent (EL) units spontaneously form without requiring a complex assembly or external electrode-based carrier injection; merely, the spatial contact between the fibers suffices. This approach effectively addresses the failure issues commonly encountered with conventional thin-film devices when applied to textiles. The inherent high-curvature loop structure of this knitted fabric effectively absorbs multi-directional deformations (strain > 100%), ensuring the stability of the light emission under stretching, bending, and pressing. Furthermore, this single textile structure successfully integrates a display module, a keyboard input interface, and a solar power supply system, thereby forming a self-contained textile-based communication tool.

The orthogonal interlacing architecture of woven fabrics establishes a highly ordered yarn grid, wherein warp and weft intersections function as primary stress concentration zones. This configuration inherently restricts yarn slippage, imposing a fundamental strain limitation typically below 20% while generating low porosity ( $\approx 30\%$ ) that constrains breathability. Crucially, these interlacing points constitute critical vulnerability sites for functional coatings—during repeated laundering, mechanical abrasion preferentially degrades conductive layers at crossover regions, manifesting as up to 150% resistance increase after 20–50 wash cycles. Strategic interventions such as post-weaving coating deposition and interlacing point reinforcement *via* microencapsulation can extend functional durability beyond 80 cycles while preserving structural integrity.

Woven fabrics offer distinct advantages for smart wearable textiles. The unique woven structure facilitates predictable conductive pathways for efficient sensing, energy harvesting, or signal transmission, while supporting scalable manufacturing *via* established weaving processes. However, limitations persist: the relatively rigid interlacing points can restrict extreme stretchability to achieve large mechanical deformability to adapt to various human movements.

#### 4.2 Knitted fabrics

In contrast to the rigid orthogonality of woven fabrics, knitted textiles derive their functionality from interlocking looped structures, offering inherent mechanical elasticity, conformability, and three-dimensional porosity. This dynamic architecture enables seamless integration of conductive fibers (*e.g.*, carbonized yarns and liquid metal-encapsulated threads) into stretchable networks, making knitwear particularly suitable for monitoring complex biomechanical movements and physiological signals in wearable applications.

Ariana Levitt *et al.*<sup>78</sup> developed a continuous coating process to uniformly deposit MXenes (51 wt% loading) onto cotton/nylon yarns, addressing the issue of high electrical resistance in long electrodes (Fig. 7a). Using an industrial knitting machine, they fabricated interlocking structured supercapacitors from the MXene-coated yarns. These devices

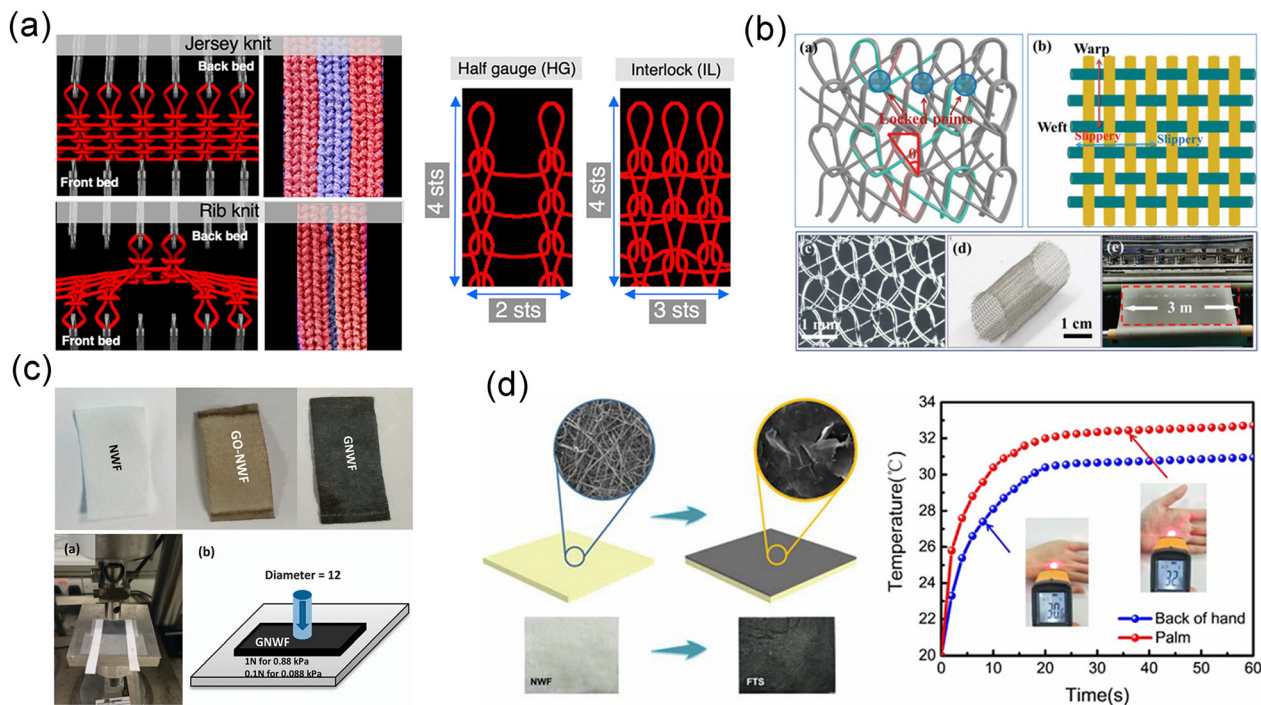


**Fig. 7** (a) Knitting process interweaves MXene-modified cotton/nylon yarns. Reproduced from ref. 78 with permission from Elsevier, copyright 2020. (b) Schematic of stainless-steel fibers (SSF) woven into a 2D interconnect network structure. Reproduced from ref. 79 with permission from John Wiley and Sons, copyright 2020. (c) Schematic of graphene-coated medical NWF and pressure test. Reproduced from ref. 80 with permission from Royal Society of Chemistry, copyright 2016. (d) Graphene/alginate NWF temperature sensor. Reproduced from ref. 81 with permission from Springer Nature, copyright 2019.

achieved an area capacitance of  $707 \text{ mF cm}^{-2}$  (at  $2 \text{ mV s}^{-1}$ ) in  $1 \text{ M H}_3\text{PO}_4$  electrolyte, demonstrated stable capacity retention over 10 000 cycles, and delivered a voltage output of  $1.5 \text{ V}$  when three devices were connected in series. Shao *et al.*<sup>79</sup> innovatively utilized stainless-steel fibers (SSFs) knitted into a 2D interconnected network structure (stainless-steel mesh, SSM) (Fig. 7b). By leveraging a loop-based knitting topology (enabled by triangular angle variations), they transformed the intrinsic angular elasticity of the metal into macroscopic stretchability. This approach successfully resolved the inherent challenge of metal materials being non-stretchable. The resulting supercapacitor exhibits exceptional stretchability ( $\geq 40\%$  strain) and mechanical stability (1000 cycles), thereby providing a robust energy solution for wearable electronics.

Knitted fabrics derive superior elasticity (100–300% strain) from their interlocking ring topology, where coil density is adjusted inversely to maximum ductility: low-density structures (5 coils per cm) achieve higher deformation thresholds but have poor dimensional recovery, while high-density structures maintain structural stability at 200% strain. The open-loop architecture provides superior air permeability ( $300\text{--}800 \text{ L m}^{-2} \text{ s}^{-1}$ ) with a porosity of  $\approx 70\%$ , but introduces a durability hole at the ring joint. Repeated washing can cause shear-driven fiber breakage at these nodes.

Knitted fabrics, characterized by interlocking loop structures, offer distinct advantages for smart textiles, primarily

their exceptional elasticity, conformability, and inherent breathability, making them ideal for comfortable, form-fitting wearable applications requiring large strain detection (*e.g.* body motion monitoring). However, this high deformability and lower structural stability can lead to potential issues like dimensional instability under loading, variability in electrical contact resistance during dynamic stretching, and challenges in precisely maintaining the geometry and alignment of integrated electronic components or rigid sensors.

#### 4.3 NWFs

Nonwoven fabrics (NWFs) are formed by consolidating short fibers of non-uniform length oriented in diverse directions. They exhibit high flexibility and foldability due to the high aspect ratio of its constituent fibers, making it suitable for electronic devices requiring bending or even stretching. Furthermore, the NWF possesses characteristics such as a simple manufacturing process, high production speed, large output, and low cost, rendering it appropriate for fabricating flexible electronic devices intended for disposable or short-term use.

Du *et al.*<sup>80</sup> employed a medical-grade NWF as a substrate, leveraging its porous fibrous network structure to achieve uniform coating of graphene (Fig. 7c). This approach enabled the fabrication of a high-sensitivity, low-cost wearable sensor, offering a novel mechanism for micro-strain monitoring (*e.g.*,

in healthcare applications). The resulting device exhibits exceptional performance metrics: high sensitivity (gauge factor:  $-7.1$  for strain; pressure sensitivity:  $0.088 \text{ kPa}^{-1}$ ), robust stability ( $>10\,000$  cycles), and biocompatibility, demonstrating significant potential for medical wearable devices. Wang *et al.*<sup>81</sup> developed a graphene/alginate NWF temperature sensor *via* dip-coating, achieving ultrahigh sensitivity (TCR =  $-1.5\% \text{ } ^\circ\text{C}^{-1}$ ), medical-grade accuracy ( $0.1 \text{ } ^\circ\text{C}$ ), and exceptional anti-interference to strain/humidity (Fig. 7d). Its capability to detect subtle skin temperature differences (*e.g.*  $0.3 \text{ } ^\circ\text{C}$  between palm and dorsum) demonstrates promising applicability in wearable health monitoring.

The stochastic fiber arrangement in nonwoven fabrics generates exceptionally high porosity (typically 80–90%) through multidirectional fiber entanglement, creating interconnected void channels that enable superior breathability ( $>800 \text{ L m}^{-2} \text{ s}^{-1}$ ) and rapid moisture transport. However, this disordered architecture intrinsically compromises mechanical integrity: weak fiber-fiber bonding interfaces allow irreversible fiber slippage under tension, limiting strain recovery to  $<60\%$  and causing permanent morphological changes beyond 30–50% elongation. Crucially, the absence of structural periodicity concentrates mechanical stress at sparse bonding points during laundering, accelerating interfacial debonding and progressive pore collapse. This structural vulnerability necessitates extensive binder integration, which conversely reduces porosity and permeability while introducing chemical degradation pathways during wet processing. Consequently, the fundamental trade-off between permeability and durability remains governed by the degree of fiber entanglement density and bonding-point distribution within the three-dimensional network.

In summary, NWF presents a compelling platform for flexible electronics due to its inherent mechanical compliance (enabling bending, folding, and potential stretching), coupled with significant manufacturing advantages including process simplicity, high production throughput, and low cost. These attributes make NWF particularly suitable for disposable or short-term use applications. However, its typically lower mechanical stability under repeated mechanical deformation compared to woven textiles remains a limitation for long-term device reliability. We systematically compared the different characteristics of the three fabrics, which is presented in Table 2.

## 5. Smart wearable applications

### 5.1 Human body signals and health monitoring

Human whole-body motion signals can provide rich health information and diverse data for comprehensive monitoring of human condition and physical rehabilitation. Traditional rigid sensors can only detect small strain behaviors and cannot accurately identify complex human body movement information. Therefore, flexible strain sensors can be installed in different parts of the human body, and the monitoring and identification of human motion signals can be realized through the different electrical signal waveforms fed back by the sensors on the strain behavior.<sup>82–84</sup> For human body motion monitoring, it is not only necessary for the sensors to have high sensitivity, but also a large strain testing range. Detecting the bending motion of the elbow and knee joints requires the strain sensor to work properly over a large monitoring range. At the same time, flexible strain sensors also enable the detection and recognition of subtle movements such as swallowing and speaking. The motion monitoring function of flexible strain sensors will play an important role in the future human applications of smart wearable electronic devices.<sup>85</sup>

Park *et al.*<sup>86</sup> integrated supercapacitors and strain sensors into a textile system consisting of liquid-metal interconnects. The system can successfully detect strains induced by joint movements and wrist pulses. It demonstrated the high feasibility of using the prepared scalable integrated textile system for real-time health monitoring of everyday wearable devices (Fig. 8a–c). Chen *et al.*<sup>87</sup> prepared a highly conductive and highly stretchable fiber PEE, which consisted of a core fiber, an intermediate modified layer, and an external eutectic gallium indium liquid metal layer. The fiber has excellent stretchability, sensitivity and wide operating range, and can be used as a smart wearable sensor to detect human behaviors including wrist, finger, elbow and knee bending. It also shows excellent thermal stability with a maximum operating temperature close to  $250 \text{ } ^\circ\text{C}$  (Fig. 8d–f). Ma *et al.*<sup>88</sup> developed an E-fabric, which consists of a conductive core jacket fabric and a spacer fabric, enabling dual pressure and strain sensing. This fabric is designed for sewing taekwondo suits that can detect tensile and pressure deformations in real combat.

**Table 2** Characteristics and applications of the three fabrics

	Woven	Knitted	Nonwoven
Structure	Yarn interweaving	Coil interlocking	Random fiber network
Porosity	Low ( $\approx 30\%$ )	Medium ( $\approx 70\%$ )	High (80–90%)
Tensile rate	5–20%	100–300%	30–50%
Compatibility	<ul style="list-style-type: none"> <li>Wet spinning</li> <li>Spray coating</li> <li>Immersion</li> <li>Magnetron sputtering</li> <li>Screen printing</li> </ul>	<ul style="list-style-type: none"> <li>Wet spinning</li> <li>Spray coating</li> <li>Immersion</li> </ul>	<ul style="list-style-type: none"> <li>Electrospinning</li> <li>Immersion</li> <li>Synthesis <i>in situ</i></li> <li>Spray coating</li> </ul>
Breathability	$50\text{--}200 \text{ L m}^{-2} \text{ s}^{-1}$	$300\text{--}800 \text{ L m}^{-2} \text{ s}^{-1}$	$>800 \text{ L m}^{-2} \text{ s}^{-1}$
Application	<ul style="list-style-type: none"> <li>Low strain sensing</li> <li>EMI shielding clothing</li> </ul>	<ul style="list-style-type: none"> <li>Large deformation monitoring</li> <li>Stretchable circuit</li> </ul>	<ul style="list-style-type: none"> <li>Biosensing</li> <li>Breathable heat management lining</li> </ul>



**Fig. 8** (a) Conceptual diagram of an integrated system for monitoring biological signals using smart fabrics sewn onto T-shirts and nylon gloves. Detection of biosignals with the strain sensor driven by a supercapacitor. Current change with (b) finger bending and (c) wrist bending. Reproduced from ref. 86 with permission from American Chemical Society, copyright 2019. (d) Schematic of the PPE fiber sensor attached to different parts for detecting human motions. Photographs and corresponding signals of the (e) bending of wrist and (f) bending of elbow. Reproduced from ref. 87 with permission from American Chemical Society, copyright 2020. (g) Schematic of the set up for carotid artery pulse measurement. Capacitance change with carotid artery pulse. (h) Schematic of the set up for the vocal cord vibration detection. Capacitance change when swallowing. Reproduced from ref. 89 with permission from John Wiley and Sons, copyright 2020. (i and j) LED in the smart textile system was set to be turned on when the electrical resistance of the integrated sensor reached a certain threshold value (yellow region). Reproduced from ref. 90 with permission from American Chemical Society, copyright 2019. (k) Manufacturing MXene-based E-skins through spray coating. Reproduced from ref. 91 with permission from Elsevier, copyright 2024.

Bennet is stripped from the e-textile and has a wide deformation range (90%) and a wide pressure detection range (110 kPa) to accurately monitor movement and morphology under large mechanical deformations. It has great potential for application in the analysis of athletic training such as taekwondo. Li *et al.*<sup>89</sup> successfully opened a GelMA-based wearable capacitive haptic sensor for monitoring human physiological signals (Fig. 8g and h). Compared with previously reported hydrogel-based pressure sensors, this GelMA sensor not only has a robust structure and reliable encapsulation performance, but also shows higher sensitivity and lower limit of detection (LOD). The high durability demonstrated in 3000 cycle tests and long-term stability when exposed to air for up to 3 days proved the success of hydrogel tactile sensors in monitoring

human physiological signals, pulse, and vocal cord vibration, encouraging their practical use in medical wearable applications. Kim *et al.*<sup>90</sup> prepared optical fiber strain sensors by *in situ* reduction of AgNPs on the surface of PU fibers (Fig. 8i and j). The initial resistance was as low as  $0.9 \Omega \text{ cm}^{-1}$ . The sensor can be sewn into a lap band to monitor the electrical signals in real time, thus helping the user to maintain proper posture during workouts. This is due to the sensor's 220% wide strain sensing range, high sensitivity ( $\sim 5.8 \times 10^4$ ) and high cycling durability (>5000 cycles). These results will provide meaningful insights for the development of the next generation of clothing-based stretchable and wearable sensors. Miao *et al.*<sup>91</sup> obtained MXene-based flexible E-skins by assembling conductive ink MXenes layer by layer on a flexible trans-

parent polyethylene terephthalate (PET) substrate *via* a spraying technique. This flexible E-skin exhibits a low thin-layer  $200 \Omega \text{ sq}^{-1}$ . In addition, the wearable E-skin based on the robust and flexible MXene-based electrode not only adapts to the mechanical deformation of the human body, but also accurately recognizes and identifies the human body's movements, including proximity, touch, and press behaviors. The sensing performance of the flexible and wearable MXene-based E-skin remains stable after more than 1000 cyclic pressing tests, which is crucial in human-computer interaction, touch panels, and personalized healthcare, and this research is promising for emerging flexible electronics and wearable applications (Fig. 8k). Zhou's team<sup>92</sup> utilized adjustable conductive cotton as the electrode/sensitive layer, combined with real-time deep learning data analysis, to achieve intelligent monitoring and recognition functionality. This sensor not only provides high sensitivity ( $6.1 \text{ kPa}^{-1}$ , with pressure below 16 kPa), a wide detection range (0–62.2 kPa), fast response and recovery times (32 ms and 48 ms, respectively), but also excellent biocompatibility and complete biodegradability. It can realize monitoring of human physiological behaviors such as gait and breathing, providing a new strategy for textile pressure sensors in next-generation smart green electronic devices. Zhang's team<sup>93</sup> used natural silk protein, ionic liquids, and glycerol as raw materials and, through continuous wet spinning technology, prepared a high-strength, conductive, and stable silk protein-based ionic hydrogel (SIH) fiber. Not only do the SIH fibers exhibit excellent mechanical strength, extensibility, and stable conductivity, but also the circuits integrated with SIH fibers can demonstrate instantaneous and characteristic responses to stimuli such as burning, immersion in water, cutting by sharp objects, and finger touch, endowing SIH fibers with sensing and protective capabilities for smart textiles. Additionally, SIH fibers retain the sustainability, biocompatibility, and biodegradability of their precursor materials, offering new perspectives for the design of next-generation smart wearable devices and the reimagining of human-machine interfaces.

Flexible wearable devices, with their high conductivity, excellent stretchability, and high sensitivity, can accurately capture changes in resistance and capacitance of wearable devices during human movement, enabling real-time continuous monitoring and recognition of subtle human movements. However, during continuous monitoring, repeated stretching and bending of wearable devices can damage the conductive pathways, leading to unstable monitoring signals. Although current wearable devices already possess high stretchability, maintaining both mechanical stability and sensitivity during long-term use remains a challenge.

## 5.2 Personal thermal management

Fabrics play an integral and important role in controlling the microclimate around the human skin as an interface for the exchange of matter and energy between the human body and its surroundings.<sup>1,2</sup> In general, thermal comfort for the human body is usually achieved by simply increasing/decreasing the

thickness of conventional clothing, but it cannot adapt to the drastic changes in ambient temperature around the human body.<sup>3,5</sup> For smart wearable electronic devices, which are closely attached to human skin, uncontrollable temperature fluctuations during long-term wear may lead to physical/psychological discomfort or even life-threatening. Meanwhile, heat is constantly generated during operation, and if the heat cannot be effectively distributed, it will accumulate, leading to thermal runaway around the human body. Meanwhile, flexible batteries sometimes encounter short-circuit problems and cause thermal runaway accidents during their use in self-powered wearable electronics. Textiles that can effectively regulate human body temperature, prevent thermal runaway, and achieve thermal comfort of the human body during the long-term wearable process have received increasing attention.<sup>9,94</sup> The following discussion focuses on thermal management textiles with smart responses, radiation cooling textiles, smart textiles based on phase change materials and Janus thermoregulation textiles (Table 3).

**5.2.1 Cooling textiles.** Based on the type of cooling, textiles with cooling function can be categorized into actively cooled textiles and passively cooled textiles.

Active cooling textiles are mainly used to improve the heat transfer rate of textiles to achieve the purpose of cooling by adding nanofillers with high thermal conductivity, such as CNTs, graphene, boron nitride (BN), transition metal carbides/nitrides (MXenes), and LMs.<sup>95–98</sup>

Gao *et al.*<sup>99</sup> prepared a personal thermal management textile based on thermally conductive and highly aligned BN/PVA fiber for personal cooling by 3D printing. The fiber has excellent mechanical strength (355 MPa), uniform thermal dispersion and high thermal conductivity (Fig. 9a). Fabrics based on a-BN/PVA fiber have a high thermal conductivity of  $0.078 \text{ W m}^{-1} \text{ K}^{-1}$ , which is 1.56 and 2.22 times higher than that of PVA and cotton fabrics, respectively. In addition, the cooling effect of the a-BN/PVA fabric was 55% higher than that of the commercial cotton fabric. This 3D printed wearable cooling textile composed of a-BN/PVA fibers provides an effective option for personal cooling of building occupants during hot weather, thereby reducing the need for indoor thermoregulation and significantly lowering the energy and cost of cooling the building itself. Song *et al.*<sup>100</sup> combined graphene/poly (ethylene glycol)/nano protofibrillated cellulose (G/PEG/NFC) to make a hybrid film that not only has shape memory and shows excellent response to stimuli, but also can change its shape in response to external stimuli. The temperature of the device is visualized by the shape change, and thermal management can be further improved by increasing the contact area of the film with air during the shape change. A five-layer G/PEG/NFC-5 hybrid film with high thermal conductivity was further developed by introducing a multilayer hybrid film combining evaporation-induced self-assembly technology and thermo-compression technology to meet the requirements of practical wearable applications, and the hybrid system can intelligently change its shape with temperature to act as a smart thermal management device for active heat dissipation.

**Table 3** Types, characteristics, and applications of personal thermal management textiles

Personal thermal management	Type	Characteristics	Application
Cooling textiles	Active cooling textiles	<ul style="list-style-type: none"> <li>• Active cooling</li> <li>• High thermal conductivity</li> <li>• Precise temperature control</li> <li>• High cooling capacity</li> </ul>	High-temperature environments, strenuous exercise and situations requiring precise temperature control.
	Radiation cooling textiles	<ul style="list-style-type: none"> <li>• Passive heat dissipation</li> <li>• No external energy required</li> <li>• High solar reflectance (in the wavelength range of 0.3 to 2.5 <math>\mu\text{m}</math>)</li> <li>• High infrared emissivity (in the wavelength range of 8 to 13 <math>\mu\text{m}</math>)</li> </ul>	Suitable for daily, outdoor, long-term and dispersed usage scenarios
Warming textiles	Joule heating of textiles	<ul style="list-style-type: none"> <li>• Requires power supply</li> <li>• Fast heating</li> <li>• High efficiency</li> <li>• Precise temperature control</li> </ul>	Suitable for rapid and uniform heating scenarios
	Photothermal heating of textiles	<ul style="list-style-type: none"> <li>• Requires light, non-contact</li> <li>• Low energy consumption</li> <li>• Low energy conversion efficiency</li> </ul>	Suitable for solar or local heating needs
Janus textiles	Janus dual mode smart textiles	<ul style="list-style-type: none"> <li>• Simultaneously provides heating and cooling</li> <li>• Wide temperature control range</li> <li>• Adaptable to multiple locations</li> </ul>	Wide range of temperature control scenarios

Radiative cooling technology, as a passive heat dissipation process that does not require any energy input, is becoming a frontier in the research of environmentally friendly cooling methods for personal thermal management. According to the principle of Kirchhoff's radiation law, textiles with high broadband emissivity will absorb significant heat from the surrounding environment. In order to effectively minimize environmental heat gain while ensuring the smooth release of heat to outer space through the atmospheric transmission window (ATW), the design of radiative cooling materials should focus on selective emission in the ATW band and efficient reflection in the non-ATW wavelength range. Typically, an efficient daytime radiative cooling process requires strong solar reflection in the 0.3–2.5  $\mu\text{m}$  wavelength range and high emissivity in the mid-infrared wavelength range (8–13  $\mu\text{m}$ ).<sup>101</sup>

Wang *et al.*<sup>102</sup> prepared camel-hair-like porous elastic fibers (MEPF) and their bilayer fabrics (MEPFT-d) using thermoplastic polyurethane (TPU) elastomers as raw materials by micro-extruded physical foaming process (Fig. 9b and c). MEPFT-d utilizes its micro- and nanoporous structure to exhibit radiative cooling capacity through high solar reflectance and emittance, exhibits low thermal conductivity, delays heat scattering, and promotes evaporative cooling through unidirectional water transport. These excellent properties ensure that MEPFT-d reduces heat loss in cold weather (7.2  $^{\circ}\text{C}$  higher than cotton) and blocks outside heat in hot weather (10.2  $^{\circ}\text{C}$  lower than cotton), making it suitable for a variety of complex outdoor scenarios. The cost-effectiveness and superior wearing comfort of this smart wearable textile provide innovative avenues for sustainable energy, smart textiles and personal thermal comfort applications. Since more than 90% of clothing is perpendicular to the ground in normal life, Wu *et al.*<sup>103</sup> explored the radiative cooling performance of textiles in a vertical state by developing a mid-infrared spectrally selective layered fabric

(SSHF) whose emissivity dominates the atmospheric transport window by molecular design, minimizing the net heat gain to the surroundings. SSHF has a high solar spectral reflectance of 0.97, which is due to the strong Mie scattering of the nano-micro hybrid fiber structure. When placed vertically in a simulated outdoor urban scene during the day, the SSHF is 2.3  $^{\circ}\text{C}$  cooler than a solar reflective broadband transmitter and also offers excellent wearability (Fig. 9d and e). Wang's team<sup>104</sup> utilized electrospinning technology with silk protein as a raw material to prepare a silk-based Janus nanofiber textile (Janus RSF) with an asymmetric micro-nano structure. This textile not only exhibits excellent heat dissipation-moisture wicking synergistic performance, high solar reflectance, infrared emissivity, and moisture-wicking quick-drying properties, making it suitable for passive cooling textiles, but also possesses biocompatibility and biodegradability. Under direct sunlight, the Janus nanofiber textile can achieve a cooling effect of nearly 9  $^{\circ}\text{C}$ , providing new insights for the development of multi-mechanism synergistic thermal and moisture management materials and low-carbon, environmentally friendly smart textiles.

**5.2.2 Warming textiles.** Based on Joule's law, Joule-heated textiles mainly utilize the heat generated when an electric current passes through a conductive material to achieve heating. With the advantages of fast warming, high efficiency and precise control, it can be used to realize rapid warming of fabrics. Photothermal heating textiles utilize the material to absorb the energy of sunlight or other light sources and convert it into heat energy, thus realizing the heating effect. It is a non-contact, precisely positioned heating method, which can be used for solar self-heating garments or localized heat therapy equipment.

Zuo *et al.*<sup>3</sup> prepared a AgNWs-MXene-PEG@ANF smart fiber with photoelectric responsive properties, which showed excellent electrical conductivity (conductivity  $2 \times 10^4 \text{ S m}^{-1}$ ), and



**Fig. 9** (a) Schematic of the thermal regulation textile. Reproduced from ref. 99 with permission from American Chemical Society, copyright 2017. (b) schematic comparison of the radiative cooling principle of MEPF with that of conventional porous fibers, (c) schematic of MEPFT thermal management mechanism. Reproduced from ref. 102 with permission from John Wiley and Sons, copyright 2024. Concept and advantages of a spectrally selective textile for vertically oriented fabrics for radiative cooling. (d) an open scenario and (e) urban scenario. Reproduced from ref. 103 with permission from American Association for the Advancement of Science, copyright 2024. (f) Light stimuli-response curves of ANFs, AgNWs-MXene@ANFs, AgNWs-MXene-PEG@ANFs and the corresponding infrared images. (g) Car model that simulated a lunar rover without batteries could continue to walk for 160 cm even after the light stimuli were removed. Reproduced from ref. 3 with permission from Elsevier, copyright 2022. (h) Photograph of a mannequin wearing a vest made of an LNT. IR image of a mannequin wearing the homemade vest after 30 min under sunlight. (i) Solar thermal heating measurement device. (j) Infrared images of fabrics, NPTFE, and cotton in a 0 °C cold environment. Reproduced from ref. 107 with permission from John Wiley and Sons, copyright 2024.

the smart fabric prepared from this smart fiber showed rapid stimulation corresponding performance under photoelectric stimulation to achieve fabric heating, while due to the addition of PCM, the smart fabric is enabled to effectively buffer temperature fluctuations and respond to external stimuli in an intelligent manner to avoid uncontrollable drastic changes in temperature (Fig. 9f and g). Yan *et al.*<sup>105</sup> deposited MXenes on a silk fabric to prepare a dual-drive heated (photovoltaic) fabric, namely MXene@silk. The surface temperature of the fabric can reach more than 80 °C within 70 s when the light intensity is 400  $\text{mW cm}^{-2}$ . The surface temperature of the fabric can reach more than 80 °C in 70 s under natural light irradiation. Under natural light, the surface temperature reaches more than 120 °C in 60 s. The fabric's surface temperature can be increased to more than 80 °C in 70 s. At the same time, due to the fabric's excellent conductivity, Joule heating can be realized, reaching 60 °C in 120 s at 10 V. Based

on the fabric's responsiveness to photoelectric stimuli, the fabric has great potential for the development of cold-weather fashion apparel and cold-proof clothing. Tao *et al.*<sup>106</sup> used thermoplastic polyurethane (TPU) and silica ( $\text{SiO}_2$ ) aerogel particles as raw materials and employed a continuous coaxial wet spinning process to prepare a multi-material aerogel composite fabric with breathability, flexibility, low thermal conductivity, and low thermal radiation properties. The fabric exhibits low thermal conductivity and infrared emissivity within the 7–14  $\mu\text{m}$  wavelength range. In a cold environment of 10 °C, the peak temperature difference between the aerogel fabric and human skin was 5.7 °C, demonstrating excellent thermal insulation performance. This provides a research direction for the development of insulating fabrics for outdoor cold environments.

As two typical important heating technologies, Joule heating and photothermal heating have their unique advan-

tages and disadvantages and application scenarios. Joule heating can realize rapid warming, but requires conductive materials and high energy consumption. Photothermal heating requires low energy consumption but has low energy conversion efficiency and is dependent on light conditions. Both show potential for application in smart wearable textiles, with Joule heating being suitable for fast and uniform heating scenarios, while photothermal heating is more suitable for solar energy utilization or localized heating needs.

**5.2.3 Janus dual mode smart textiles.** Integrating radiant cooling and heating modes together seamlessly in the same fabric for freely switchable cooling and heating for complex fluctuating environments is an ideal solution.

Cheng *et al.*<sup>107</sup> developed a breathable bimodal leather-like nanotextile (LNT) with asymmetric wrinkled photonic microstructures and Janus wettability for efficient personal thermal management by one-step electrostatic spinning. The resulting LNT exhibits efficient cooling (22.0 °C) and heating (22.1 °C) capabilities in sunlight (28.3 °C wider than typical textiles). In addition, it has good breathability, softness, stretch and sweat absorption. Practical tests have shown that the LNT can provide a comfortable micro-environment for the body in changing weather conditions (1.6–8.0 °C lower and 1.0–7.1 °C warmer than typical textiles). This wearable bimodal LNT brings great potential for personal thermal comfort and opens up new possibilities for all-weather smart clothing (Fig. 9h–j). Luo *et al.*<sup>108</sup> simultaneously realized cooling and heating functionalities by assembling a sandwich architecture that combines a solar-heating, high-emissivity reduced-graphene-oxide (RGO) layer, a visibly-transparent polydimethylsiloxane support coating, and a spectrally-selective nanoporous polytetrafluoroethylene radiative-cooling substrate, enabling multi-scenario personal thermal management. The resulting hyperstructured fabrics exhibited spectrally selective, high solar spectral reflectance (>90%) in the range of 0.25–2.5 μm and high transparency (>90%) in the range of 7–14 μm human infrared radiation. At an ambient temperature of 36 °C, the hyperstructured fabric can not only dissipate thermal radiation from the skin, but also block solar radiation heat through the outermost visible reflective nanoporous PTFE layer, which can achieve a radiative cooling down temperature of 3.2 °C compared with traditional cotton fabrics. For solar heating, the hyperfabric converts solar radiation into heat through the outer RGO layer, maintaining a warmer surface microclimate, 17.0 °C higher than conventional cotton in a cold environment at 0 °C. By flipping the front and back sides of the hyperfabric, it is easy to switch between radiant cooling and solar heating modes, which can be adapted to a wide range of scenarios for efficient thermal management. Tao *et al.*<sup>109</sup> prepared a versatile coating with superhydrophobicity and adaptive temperature regulation using a phase separation process. The coating has an asymmetric gradient structure, with hydrophobic silica (SiO<sub>2</sub>) particles embedded in the surface and thermochromic microcapsules embedded in the subsurface. The coating exhibits high infrared emissivity and thermally switchable solar reflectance, enabling radiative cooling at high temperatures

and solar heating at low temperatures, thereby achieving autonomous temperature regulation. Additionally, the coating possesses superhydrophobicity and self-cleaning properties, opening new prospects for the manufacturing and application of smart temperature-controlled coatings.

Smart-responsive thermal management textiles are crucial for maintaining a stable microclimate around the human body. Based on varying thermal needs, currently developed personal thermal management smart wearable textiles primarily include cooling textiles, warming textiles, and Janus dual-mode smart textiles. Cooling and warming textiles regulate temperature in response to single environmental changes, while Janus dual-mode smart textiles can adapt to more complex environmental fluctuations. In addition to achieving temperature regulation performance, the fabric should prioritize comfort and long-term stability, achieving low energy consumption and precise temperature control to withstand extreme environmental changes.

### 5.3 Electromagnetic shielding

With the proliferation of electronic devices, EMI shielding in wearable textiles is critical to protect humans from harmful radiation and ensure device reliability. Nanomaterials with high conductivity and tunable structures are ideal for lightweight flexible EMI shielding textiles. EMI shielding textiles can be used in a wide range of civil protection, industrial and military applications. The shielding principles include reflection loss, absorption loss and multiple reflection loss, which are achieved through conductive fibers (*e.g.* metal fibers and carbon nanotube fibers), conductive polymers or composites. The preparation of high-performance, intelligently responsive and multifunctionally integrated electromagnetic shielding fabrics can meet the needs of a wider range of application scenarios.

Yang *et al.*<sup>110</sup> successfully chemically anchored CNTs and silver-coated nylon 6 (Ag@PA6) onto poly(vinyl alcohol-*co*-polyethylene) (PVA-*co*-PE) nanofibers by vacuum filtration, chemical crosslinking, and ultraviolet cross-linking modification and successfully prepared PVA/CNTs/PA6 composite thin films with a multistage cross-linking-enhanced structure. The composite film can achieve high EMI SE at low dielectric filling, the maximum loss of incident electromagnetic wave reaches 42.5 dB, and the EMI SSE/t reaches 11 100.5 dB cm<sup>2</sup> g<sup>-1</sup>. This special multistage composite reinforcement network structure not only has satisfactory impedance/magnetic matching, dielectric loss, interfacial polarization, and internal multiple reflection scattering, but also shows excellent performance in terms of impedance/magnetic matching and interface polarization. This special multilevel composite reinforcement network structure not only has satisfactory impedance/magnetic matching, dielectric loss, interface polarization, and internal multiple reflection scattering but also exhibits excellent thermal management, infrared shielding, non-flammability, and mechanical properties. This study has potential for practical application in the development of EMI shielding protection in flexible wearable electronics (Fig. 10a). Niu *et al.*<sup>111</sup>



**Fig. 10** (a) Schematic of the PVA/CNTs/PA6 film. Reproduced from ref. 109 with permission from John Wiley and Sons, copyright 2024. (b) Schematic of the EMI shielding mechanism of (MXene@Ni/PNF) (MXene/PNF) aerogels when electromagnetic waves are incident from the absorbent layer of MXene@Ni/PNF. Reproduced from ref. 111 with permission from Elsevier, copyright 2025. (c) Schematic of the device used to generate continuous fiber lithium-ion batteries. (d) Fiber lithium-ion battery fabric provides wireless charging for smartphones. Reproduced from ref. 114 with permission from John Wiley and Sons, copyright 2022. (e) Schematic and application demonstration of F-TENGs. F-TENG monitoring (f) normal breathing and (g) normal meditation. Reproduced from ref. 118 with permission from Royal Society of Chemistry, copyright 2022.

prepared MXene/Ag nanocomposites using an *in situ* self-reducing method, and a novel silver-based hybrid nanoparticle ink (MXene/Ag–Ag) for conformal EMI shielding application was prepared by designing a solvent system. The prepared MXene/Ag–Ag film achieved an EMI shielding efficiency of more than 99% with a specific shielding effectiveness (SSE/*t*) as high as 52 591.4 dB cm<sup>2</sup> g<sup>-1</sup> at a thickness of only 500 nm and a weight of only 0.9 mg. This study provides a new approach for the development of the next-generation of lightweight and integrated electronics with high EMI shielding performance. Liu *et al.*<sup>112</sup> prepared PNFs by a deprotonation method, successfully grew Ni nanoparticles *in situ* on the surface of MXenes to prepare heterostructured MXene@Ni EM functional fillers, and adjusted the EM parameters of the functional fillers to achieve a good impedance matching performance in the X-band. When the mass ratio of MXene to Ni is 1/6, MXene@Ni exhibits the best EM absorption loss capability in the X-band. The absorbing layer of MXene@Ni/PNF has good

impedance matching and absorption loss capability for EM waves, and the reflective layer of MXene/PNF ensures the assembly (MXene@Ni/PNF) due to its high electrical conductivity, the reflective layer of MXene/PNF guarantees the excellent EMI shielding performance of the assembled (MXene@Ni/PNF) aerogel due to its high conductivity. When the mass fraction of MXenes in the MXene/PNF reflective layer is 80 wt%, the average EMI SE of the (MXene@Ni/PNF)-(MXene/PNF) aerogel in the X-band is 71 dB, the average EMI SER is as low as 0.5 dB, and the average R-value of the aerogel is as low as 0.10. In addition, the assembled composite has good IR camouflage properties, enabling high infrared camouflage performance, and this EMI shielding composite material with low reflection characteristics and infrared camouflage has a broad application prospect in the next-generation smart wearable electronic devices (Fig. 10b).

Flexible wearable textiles primarily achieve electromagnetic shielding performance by adjusting the fabric structure to

create an efficient conductive network. Currently, various nanomaterials have been used to enhance the fabric conductivity and achieve electromagnetic shielding (e.g., metallic materials exhibit excellent conductivity but poor mechanical flexibility; conductive polymers have good formability but generally inferior performance; and carbon materials, metallic nanomaterials and MXene aid in constructing efficient conductive networks but are relatively costly). However, the oxidation of conductive materials and repeated stretching and bending of the fabric's conductive structure can lead to changes in resistance, thereby reducing the shielding performance. Therefore, achieving stable electromagnetic shielding performance, excellent breathability, stretchability, and long-term wearability with biological safety remains a challenge.

#### 5.4 Energy storage

In order to achieve long-term high stability and reliable operation of flexible/wearable electronic devices, and to reduce the problems of energy dissipation and frequent charging due to the constant operation of wearable electronic devices, wearable products that can provide a continuous supply of energy to wearable electronic devices and systems have attracted widespread attention. The main method of energy harvesting and storage involves the use of emerging triboelectric nanogenerators (TENGs), solar cells, lithium batteries, supercapacitors and other hybrid power generation and conversion devices.<sup>113–115</sup> Combining traditional clothing with flexible energy harvesting and storage devices not only allows for a variety of working modes, light weight, low cost, material-free operation, and high conversion efficiency, but also provides excellent wearing comfort, breathability, and other characteristics.<sup>116,117</sup>

Clothing-based TENGs can convert ambient mechanical energy from daily human activities into electrical energy, and are considered as ideal candidates for sustainable and portable power sources. Clothing-based solar cells can collect solar radiation and convert it into electricity to power wearable electronic devices during outdoor activities. However, clothing-based lithium batteries and supercapacitors with high energy/power densities can store electricity into batteries/fabrics to avoid conventional bulky energy storage devices. The combination of clothing-based energy harvesting and storage devices can provide efficient 24/7 continuous power supply, as it can readily harvest energy from the surrounding environment while storing it in the clothing.<sup>118</sup>

Fiber batteries, typical flexible energy storage devices, can be woven into textiles, providing a portable way of powering wearable electronic devices. He *et al.*<sup>115</sup> optimized the fabrication process by winding lithium cobalt oxide positive electrodes and diaphragm-wrapped negative electrodes together in order to produce a high-performance long diaphragm lithium-ion battery (FLIB) (Fig. 10c and d). The energy density of the produced FLIB was  $85.69 \text{ W h kg}^{-1}$ , and the capacity retention rate reached 90.5% after 500 charging and discharging cycles. Thanks to the protective layer, the FLIB worked even under washing and puncture conditions. The researchers have not only woven FLIBs into large-area textiles *via* rapier looms, but

also prepared it into jackets that can be used to power electronic devices and for personal health management, and the realization of such large-scale batteries holds great promise for self-powered clothing-based wearable electronics. Endogenous electrical nanogenerators (TENGs) allow for real-time physiological monitoring, but they are usually complex to fabricate, have low sensitivity, and are susceptible to interference from environmental humidity. Therefore, Shi *et al.*<sup>119</sup> developed an integrated fabric-based friction electric nanogenerator (F-TENG) using waterborne polyurethane (WPU) as a water-proof encapsulation and friction layer and polypyrrole (PPy) as a friction and conductive layer. The microfilament structure achieves localized contact separation during deformation, which triggers the friction electric effect, while the 3D architecture achieves localized strain, which further enhances the sensitivity to weak signals. The F-TENG demonstrates effective voltage output during carotid artery and respiration monitoring, highlighting its ability to detect subtle physiological signals. In addition, the F-TENG could maintain stable performance not only under humid conditions, but also when the relative humidity increased from 20% to 80%, its output voltage was maintained at 78.78%. When implanted into a humid environment in the leg of a rat, the output of the F-TENG was significantly 21 V. It also exhibited antimicrobial properties, making it promising for applications in dynamic monitoring, wearable electronic devices, and integrated diagnostic and therapeutic systems (Fig. 10e–g).

By integrating textiles with energy harvesting and storage devices, it is possible to convert energy from the human body and its surrounding environment (such as solar energy, thermal energy, mechanical energy, and electromagnetic energy) into electrical energy and power outdoor wearable devices. While current textile-based energy storage and harvesting devices possess energy harvesting and storage capabilities, they suffer from low energy storage density, low energy conversion efficiency, and poor durability. Additionally, highly conductive fibers and encapsulation layers are prone to oxidation and corrosion in air, leading to a decline in fabric performance. Furthermore, the production cost of energy storage textiles is high, and there is a risk of thermal runaway.

## 6. Summary and perspectives

This review provides not only an account of smart materials, properties, fiber fabrication strategies, surface modification, and wearable applications of smart fibers/textiles, but also a comprehensive summary of the recent advances in smart wearable fibers and textiles. Smart wearable fibers and textiles take advantage of the unique properties of intelligent nanomaterials (e.g., high sensitivity, flexibility, and electrical conductivity) and show great potential for health monitoring, human-computer interaction, and other wearable applications. These properties enable smart wearable devices to closely fit the human body, monitor physiological signals in real time, provide a comfortable wearing experience, and enable efficient

energy management. Their applications cover personal health-care, robotics, thermal management, energy harvesting and storage, and environmental monitoring. In addition, some new intelligent wearable fields need to be further expanded. For instance, fabrics with embedded biosensors required to be developed, which could track vitals (ECG, glucose, and hydration) in real time, enabling early disease detection and personalized care. In addition, smart fibers and textiles for entertainment and leisure applications need further development, such as color-shifting fabrics, touch screen-integrated designs, and shape-memory textiles.

However, smart wearable fibers and textiles are still facing a number of challenges. Wearable comfort, breathability, and human compatibility need to be emphasized as inevitable trends in the development of smart fabrics during long-term wear. Meanwhile, when integrating intelligent nanomaterials into wearable devices, not only the basic properties of nanomaterials, but also the abrasion resistance, stretchability, and water washing resistance of smart fabrics should be taken into account in order to prepare multifunctional, durable, and user-friendly practical wearable textiles.

At present, most smart wearable fibers and textiles are still in the laboratory stage, and further breakthroughs are urgently required for commercial applications: (1) first, they are limited by the fine processing and fabrication process of smart fibers and textiles, and some are only proof-of-concept demonstrations. Their seamless compatibility with modern textile processing technology still needs to be overcome by many technical difficulties. (2) Second, the current development of smart wearable fibers and textiles is mostly based on small samples, and further consideration is needed for their manufacturing costs for large-scale commercial applications. (3) Furthermore, the “killer application” of smart wearable fibers and textiles needs further exploration to make it a necessity rather than a choice in our daily life, increasing the stickiness of consumers and experiencers towards it.

Smart wearable fibers and textiles will evolve from connected to cognitive, with AI-driven fabrics anticipating needs. AI-driven textiles transcend “wearables”, and they become predictive partners enhancing human capability, health, and sustainability while blending invisibly into daily life. Convergence with nanotechnology, IoT, soft electronics, physiology, synthetic biology, and 5G will unlock applications such as textiles interfacing with neural signals. As tech becomes invisible and sustainable, smart fibers and textiles will redefine not only just wearables, but also how we interact with our surrounding environment. This shift positions textiles not only as passive coverings on human body, but also as active, responsive systems integral to human health, sustainability, and digital life.

## Conflicts of interest

The authors declare that they have no known competing financial interests or personal relationships that could have appeared to influence the work reported in this paper.

## Data availability

No primary research results, software or code has been included and no new data were generated or analysed as part of this review.

## Acknowledgements

This work was supported by the Natural Science Foundation of China (no. 52203061, 52303060), the Natural Science Foundation of Shandong Province (no. ZR2020QE081, ZR2023QB046), the Taishan Scholar Program of Shandong Province in China (tsqn202211116), the Youth Innovation Science and Technology Plan of Shandong Province (2020KJA013), the Opening Project of Textile Ecological Dyeing and Finishing Key Laboratory of Sichuan Province (Chengdu Textile College) (2024DF-A01), Young Talent of Lifting Engineering for Science and Technology in Shandong Province (Grant SDAST2024QTA066), and the University Synergy Innovation Program of Anhui Province (no. GXXT-2023-096).

## References

- 1 A. Yang, L. Cai, R. Zhang, J. Wang, P.-C. Hsu, H. Wang, G. Zhuo, J. Xu and Y. Cui, Thermal Management in Nanofiber-Based Face Mask, *Nano Lett.*, 2017, **17**, 3506–3510.
- 2 P.-C. Hsu, X. Liu, C. Liu, X. Xie, H. Lee, A. J. Welch, T. Zhao and Y. Cui, Personal Thermal Management by Metallic Nanowire-Coated Textile, *Nano Lett.*, 2015, **15**, 365–371.
- 3 X. Zuo, T. Fan, L. Qu, X. Zhang and J. Miao, Smart multi-responsive aramid aerogel fiber enabled self-powered fabrics, *Nano Energy*, 2022, **101**, 107559.
- 4 G. Wang, J. Miao, X. Ma, C.-W. Lou, J.-H. Lin, Y.-Z. Long, S. Ramakrishna and T. Fan, Robust multifunctional rGO/MXene@PPS fibrous membrane for harsh environmental applications, *Sep. Purif. Technol.*, 2022, **302**, 122014.
- 5 H. Wang, Y. Zhang, X. Liang and Y. Zhang, Smart Fibers and Textiles for Personal Health Management, *ACS Nano*, 2021, **15**, 12497–12508.
- 6 X. Zhang, W. Yang, Z. Shao, Y. Li, Y. Su, Q. Zhang, C. Hou and H. Wang, A Moisture-Wicking Passive Radiative Cooling Hierarchical Metafabric, *ACS Nano*, 2022, **16**, 2188–2197.
- 7 X. Liu, J. Miao, Q. Fan, W. Zhang, X. Zuo, M. Tian, S. Zhu, X. Zhang and L. Qu, Recent Progress on Smart Fiber and Textile Based Wearable Strain Sensors: Materials, Fabrications and Applications, *Adv. Fiber Mater.*, 2022, **4**, 361–389.
- 8 X. Ma, A. Wang, J. Miao and T. Fan, 2D lamellar membrane with MXene hetero-intercalated small sized graphene oxide for harsh environmental wastewater treatment, *Sep. Purif. Technol.*, 2023, **311**, 123248.

- 9 X. Zuo, X. Zhang, L. Qu and J. Miao, Smart Fibers and Textiles for Personal Thermal Management in Emerging Wearable Applications, *Adv. Mater. Technol.*, 2023, **8**, 2201137.
- 10 Q. Xu, J. Chen, J. R. Loh, H. Zhong, K. Zhang, J. Xue and W. S. V. Lee, Fiber-shaped batteries towards high performance and perspectives of corresponding integrated powerful textiles, *Adv. Energy Mater.*, 2023, **14**, 2302536.
- 11 W. Zhang, J. Miao, X. Zuo, X. Zhang and L. Qu, Weaving a magnificent world: 1D fibrous electrodes and devices for stretchable and wearable electronics, *J. Mater. Chem. C*, 2022, **10**, 14027–14052.
- 12 L. L. Zhu, W. Y. Zhang, Sh. Luan, J. Q. Wei, Y. Yang and J. L. Miao, Nanomaterials for smart wearable fibers and textiles: A critical review, *iScience*, 2025, **28**, 113126.
- 13 X. Han, X. Yang, Z. Sun, M. Du, Y. Du, T. Zhang and K. Zhang, A General Design Framework of Flexible Thermoelectric Devices Bridging Power Requirements for Wearable Electronics, *Mater. Today Phys.*, 2024, **46**, 101530.
- 14 Y. Zhao, J. Wang, Z. Li, X. Zhang, M. Tian, X. Zhang, X. Liu, L. Qu and S. Zhu, Washable, durable and flame retardant conductive textiles based on reduced graphene oxide modification, *Cellulose*, 2019, **27**, 1763–1771.
- 15 J. Miao and T. Fan, Flexible and stretchable transparent conductive graphene-based electrodes for emerging wearable electronics, *Carbon*, 2023, **202**, 495–527.
- 16 J. Park, J. C. Hwang, G. G. Kim and J.-U. Park, Flexible electronics based on one-dimensional and two-dimensional hybrid nanomaterials, *InfoMat*, 2020, **2**, 33–56.
- 17 G. Chen, Y. Li, M. Bick and J. Chen, Smart Textiles for Electricity Generation, *Chem. Rev.*, 2020, **120**, 3668–3720.
- 18 Y. Cai, J. Shen, C.-W. Yang, Y. Wan, H.-L. Tang, A. A. Aljarb, C. Chen, J.-H. Fu, X. Wei and V. Tung, Mixed-dimensional MXene-hydrogel heterostructures for electronic skin sensors with ultrabroad working range, *Sci. Adv.*, 2020, **6**, eabb5367.
- 19 Z. Lou, L. Wang, K. Jiang, Z. Wei and G. Shen, Reviews of wearable healthcare systems: Materials, devices and system integration, *Mater. Sci. Eng., R*, 2020, **140**, 100523.
- 20 W. Jayathilaka, K. Qi, Y. Qin, A. Chinnappan, W. Serramo, C. Baskar, H. Wang, J. He and S. Cui, Significance of Nanomaterials in Wearables: A Review on Wearable Actuators and Sensors, *Adv. Mater.*, 2019, **31**, 1805921.
- 21 L. Wang, M. Tian, Y. Zhang, F. Sun, X. Qi, Y. Liu and L. Qu, Helical core-sheath elastic yarn-based dual strain/humidity sensors with MXene sensing layer, *J. Mater. Sci.*, 2020, **55**, 6187–6194.
- 22 J. Zhang, W. Liu, M. Du, Q. Xu, M. Hung, R. Xiang, M. Liao, X. Wang, B. Wang, A. Yu and K. Zhang, Kinetic Investigation of Energy Storage Process in Graphene Fiber Supercapacitors: Unraveling Mechanisms, Fabrications, Property Manipulation, and Wearable Applications, *Carbon Energy*, 2025, **7**, e625.
- 23 F. Wang, J. Jiang, F. Sun, L. Sun, T. Wang, Y. Liu and M. Li, Flexible wearable graphene/alginate composite non-woven fabric temperature sensor with high sensitivity and anti-interference, *Cellulose*, 2019, **27**, 2369–2380.
- 24 C. You, W. Qin, Z. Yan, Z. Ren, J. Huang, J. Li, W. Chang, W. He, K. Wen, S. Yin, X. Zhou and Z. Liu, Highly improved water tolerance of hydrogel fibers with a carbon nanotube sheath for rotational, contractile and elongational actuation, *J. Mater. Chem. A*, 2021, **9**, 10240–10250.
- 25 Q. Ke, Y. Zhang, Y. Fu, C. Yang, F. Wu, Z. Li, Y. Wei and K. Zhang, Study on Electrochemical Performance of MnO@rGO/Carbon Fabric-Based Wearable Supercapacitors, *Materials*, 2023, **16**, 4687.
- 26 X. Chen, Y. He, M. Tian, L. Qu, T. Fan and J. Miao, Core-Sheath Heterogeneous Interlocked Conductive Fiber Enables Smart Textile for Personalized Healthcare and Thermal Management, *Small*, 2024, **20**, 2308404.
- 27 Q. Yang, Z. Xu, B. Fang, T. Huang, S. Cai, H. Chen, Y. Liu, K. Gopalsamy, W. Gao and C. Gao, MXene/graphene hybrid fibers for high performance flexible supercapacitors, *J. Mater. Chem. A*, 2017, **5**, 22113–22119.
- 28 B. Wei, H. Wang, M. Tian, L. Qu and S. Zhu, The graphene-polyurethane foam-coated fabric with excellent photo-thermal property, *Mater. Lett.*, 2023, **333**, 133566.
- 29 X. Liang, M. Zhu, H. Li, J. Dou, M. Jian, K. Xia, S. Li and Y. Zhang, Hydrophilic, Breathable, and Washable Graphene Decorated Textile Assisted by Silk Sericin for Integrated Multimodal Smart Wearables, *Adv. Funct. Mater.*, 2022, **32**, 2200162.
- 30 P. Tang, Z. Deng, Y. Zhang, L.-X. Liu, Z. Wang, Z.-Z. Yu and H.-B. Zhang, Tough, Strong, and Conductive Graphene Fibers by Optimizing Surface Chemistry of Graphene Oxide Precursor, *Adv. Funct. Mater.*, 2022, **32**, 2112156.
- 31 T. Yamada, Y. Hayamizu, Y. Yamamoto, Y. Yomogida, A. Lzadi-Najafabadi, D. N. Futaba and K. Hata, A stretchable carbon nanotube strain sensor for human-motion detection, *Nat. Nanotechnol.*, 2011, **6**, 296–301.
- 32 Z. Lu, J. Foroughi, C. Wang, H. Long and G. G. Wallace, Superelastic Hybrid CNT/Graphene Fibers for Wearable Energy Storage, *Adv. Energy Mater.*, 2018, **8**, 1702047.
- 33 P. Hu, J. Lyu, C. Fu, W.-B. Gong, J. Liao, W. Lu, Y. Chen and X. Zhang, Multifunctional Aramid Nanofiber/Carbon Nanotube Hybrid Aerogel Films, *ACS Nano*, 2020, **14**, 688–697.
- 34 Y. Gao, F. Guo, P. Cao, J. Liu, D. Li, J. Wu, N. Wang, Y. Su and Y. Zhao, Winding-Locked Carbon Nanotubes/Polymer Nanofibers Helical Yarn for Ultra-stretchable Conductor and Strain Sensor, *ACS Nano*, 2020, **14**, 3442–3450.
- 35 S. Jiang, H. Zhang, S. Song, Y. Ma, J. Li, G. H. Lee, Q. Han and J. Liu, Highly Stretchable Conductive Fibers from Few-Walled Carbon Nanotubes Coated on Poly(m-phenylene isophthalamide) Polymer Core/Shell Structures, *ACS Nano*, 2015, **9**, 10252–10257.
- 36 Y. R. Lee, H. Kwon, D. H. Lee and B. Y. Lee, Highly flexible and transparent dielectric elastomer actuators using silver nanowire and carbon nanotube hybrid electrodes, *Soft Matter*, 2017, **13**, 6390–6395.

- 37 G. Wang, L. Hao, X. Zhang, S. Tan, M. Zhou, W. Gu and G. Ji, Flexible and transparent silver nanowires/biopolymer film for high-efficient electromagnetic interference shielding, *J. Colloid Interface Sci.*, 2022, **607**, 89–99.
- 38 Y. Jia, C. Chen, D. Jia, S. Li, S. Ji and C. Ye, Silver Nanowire Transparent Conductive Films with High Uniformity Fabricated via a Dynamic Heating Method, *ACS Appl. Mater. Interfaces*, 2016, **8**, 9865–9871.
- 39 D. Li, W.-Y. Lai, Y.-Z. Zhang and W. Huang, Printable Transparent Conductive Films for Flexible Electronics, *Adv. Mater.*, 2018, **30**, 1704738.
- 40 Y. Lu, J. Jiang, S. Yoon, K.-S. Kim, J.-H. Kim, S. Park, S.-H. Kim and L. Piao, High-Performance Stretchable Conductive Composite Fibers from Surface-Modified Silver Nanowires and Thermoplastic Polyurethane by Wet Spinning, *ACS Appl. Mater. Interfaces*, 2018, **10**, 2093–2104.
- 41 Q. Fan, J. Miao, X. Liu, X. Zuo, W. Zhang, M. Tian, S. Zhu, L. Qu and X. Zhang, Biomimetic Hierarchically Silver Nanowire Interwoven MXene Mesh for Flexible Transparent Electrodes and Invisible Camouflage Electronics, *Nano Lett.*, 2022, **22**, 740–750.
- 42 Y. Han, K. Ruan and J. Gu, Multifunctional Thermally Conductive Composite Films Based on Fungal Tree-like Heterostructured Silver Nanowires@Boron Nitride Nanosheets and Aramid Nanofibers, *Angew. Chem., Int. Ed.*, 2023, **62**, e202216093.
- 43 R. Ma, B. Kang, S. Cho, M. Choi and S. Baik, Extraordinarily High Conductivity of Stretchable Fibers of Polyurethane and Silver Nanoflowers, *ACS Nano*, 2015, **9**, 10876–10886.
- 44 C. Wan, Y. Liu, X. Li, H. Xu, R. Guo and J. Liu, Interfacial adhesion effects of liquid metal printed electronics on general substrates: Mechanisms and applications, *InfoMat*, 2025, e70029.
- 45 H. Jiang, B. Yuan, H. Guo, F. Pan, F. Meng, Y. Wu, X. Wang, L. Ruan, S. Zheng, Y. Yang, Z. Xiu, L. Li, C. Wu, Y. Gong, M. Yang and W. Liu, Malleable, printable, bondable, and highly conductive MXene/liquid metal plasticine with improved wettability, *Nat. Commun.*, 2024, **15**, 6138.
- 46 H. Wang, B. Yuan, X. Zhu, X. Shan, S. Chen, W. Ding, Y. J. Cao, K. Dong and J. Liu, Multi-stimulus perception and visualization by an intelligent liquid metal-elastomer architecture, *Sci. Adv.*, 2024, **10**, eadp5215.
- 47 I.-A. Pavel, S. Lakard and B. Lakard, Flexible Sensors Based on Conductive Polymers, *Chemosensors*, 2022, **10**, 97.
- 48 X. Guo and A. Facchetti, The journey of conducting polymers from discovery to application, *Nat. Mater.*, 2020, **19**, 922–928.
- 49 Y. Wang, A. Liu, Y. Han and T. Li, Sensors based on conductive polymers and their composites: a review, *Polym. Int.*, 2020, **69**, 7–17.
- 50 Y. He, Q. Liu, M. Tian, X. Zhang, L. Qu, T. Fan and J. Miao, Highly conductive and elastic multi-responsive phase change smart fiber and textile, *Compos. Commun.*, 2023, **44**, 101772.
- 51 Z. Wen, Y. Yang, N. Sun, G. Li, Y. Liu, C. Chen, J. Shi, L. Xie, H. Jiang, D. Bao, Q. Zhou and X. Sun, A Wrinkled PEDOT:PSS Film Based Stretchable and Transparent Triboelectric Nanogenerator for Wearable Energy Harvesters and Active Motion Sensors, *Adv. Funct. Mater.*, 2018, **28**, 1803684.
- 52 Z. Zhu, C. Liu, F. Jiang, J. Liu, G. Liu, X. Ma, P. Liu, R. Huang, J. Xu and L. Wang, Flexible fiber-shaped hydrogen gas sensor via coupling palladium with conductive polymer gel fiber, *J. Hazard. Mater.*, 2021, **411**, 125008.
- 53 X. Li, H. Hu, T. Hua, B. Xu and S. Jiang, Wearable strain sensing textile based on one-dimensional stretchable and weavable yarn sensors, *Nano Res.*, 2018, **11**, 5799–5811.
- 54 Y. He, S. Guo, X. Zhang, L. Qu, T. Fan and J. Miao, Ultrathin two-dimensional membranes by assembling graphene and MXene nanosheets for high-performance precise separation, *J. Mater. Chem. A*, 2024, **12**, 30121–30168.
- 55 F. Guan, Y. Xie, H. Wu, Y. Meng, Y. Shi, M. Gao, Z. Zhang, S. Chen, Y. Chen, H. Wang and Q. Pei, Silver Nanowire-Bacterial Cellulose Composite Fiber-Based Sensor for Highly Sensitive Detection of Pressure and Proximity, *ACS Nano*, 2020, **14**, 15428–15439.
- 56 H. Yu, Y. Tian, M. Dirican, D. Fang, C. Yan, J. Xie, D. Jia, Y. Liu, C. Li, M. Cui, H. Liu, G. Chen, X. Zhang and J. Tao, Flexible, transparent and tough silver nanowire/nanocellulose electrodes for flexible touch screen panels, *Carbohydr. Polym.*, 2021, **273**, 118539.
- 57 X. Liu, J. Miao, Q. Fan, W. Zhang, X. Zhang, X. Zuo, M. Tian, S. Zhu, X. Zhang and L. Qu, Smart Textile Based on 3D Stretchable Silver Nanowires/MXene Conductive Networks for Personal Healthcare and Thermal Management, *ACS Appl. Mater. Interfaces*, 2021, **13**, 56607–56619.
- 58 Q. Liu, Z. Liu, C. Li, K. Xie, P. Zhu, B. Shao, J. Zhang, J. Yang, J. Zhang, Q. Wang and C. F. Guo, Highly Transparent and Flexible Iontronic Pressure Sensors Based on an Opaque to Transparent Transition, *Adv. Sci.*, 2020, **7**, 2000348.
- 59 Z. Hou, Y. He, L. Qu, X. Zhang, T. Fan and J. Miao, Core-Sheath Heterogenous Interlocked Stretchable Conductive Fiber Induced by Adhesive MXene Modulated Interfacial Soldering, *Nano Lett.*, 2024, **24**, 15142–15150.
- 60 Y. Zheng, Y. Wang, J. Zhao and Y. Li, Electrostatic Interfacial Cross-Linking and Structurally Oriented Fiber Constructed by Surface-Modified 2D MXene for High-Performance Flexible Pseudocapacitive Storage, *ACS Nano*, 2023, **17**, 2487–2496.
- 61 Y. Cheng, Y. Ma, L. Li, M. Zhu, Y. Yue, W. Liu, L. Wang, S. Jia, C. Li, T. Qi, J. Wang and Y. Gao, Bioinspired Microspines for a High-Performance Spray  $\text{Ti}_3\text{C}_2\text{T}_x$  MXene-Based Piezoresistive Sensor, *ACS Nano*, 2020, **14**, 2145–2155.
- 62 Y. He, S. Guo, L. Qu, X. Zhang, T. Fan and J. Miao, Oriented Assembly and Bridging of 2D Nanosheets

- Enabled High-Performance MXene Composite Fiber via Dual-Spatially Confined Spinning, *Adv. Funct. Mater.*, 2025, **24**, 2419923.
- 63 X. Fan, Y. Ding, Y. Liu, J. Liang and Y. Chen, Plasmonic  $Ti_3C_2T_x$  MXene Enables Highly Efficient Photothermal Conversion for Healable and Transparent Wearable Device, *ACS Nano*, 2019, **13**, 8124–8134.
- 64 A. B. Appiagyei, J. Banua and J. I. Han, Flexible and patterned-free Ni/NiO-based temperature device on cylindrical PET fabricated by RF magnetron sputtering: Bending and washing endurance tests, *J. Ind. Eng. Chem.*, 2021, **100**, 372–382.
- 65 M. Li, Y. Wang, X. Fan, H. Huang, Y. Wan, Y. Li, J. Fang, J. Gao, Y. Yang and J. Liu, A Conductive Bamboo Fabric with Controllable Resistance for Tailoring Wearable Sensors, *ACS Appl. Mater. Interfaces*, 2022, **14**, 26958–26969.
- 66 H. Wu, Y. Xie, Y. Ma, B. Zhang, B. Xia, P. Zhang, W. Qian, D. He, X. Zhang, B.-W. Li and C.-W. Nan, Aqueous MXene/Xanthan Gum Hybrid Inks for Screen-Printing Electromagnetic Shielding, Joule Heater, and Piezoresistive Sensor, *Small*, 2022, **18**, 2107087.
- 67 F. Xie, K. Gao, L. Zhou, F. Jia, Q. Ma and Z. Lu, Robust  $Ti_3C_2T_x$ /RGO/ANFs hybrid aerogel with outstanding electromagnetic shielding performance and compression resilience, *Composites, Part A*, 2022, **160**, 107049.
- 68 Y. Yang, C. Yao, W.-Y. Huang, C.-L. Liu and Y. Zhang, Wearable Sensor Based on a Tough Conductive Gel for Real-Time and Remote Human Motion Monitoring, *ACS Appl. Mater. Interfaces*, 2024, **16**, 11957–11972.
- 69 A. Wang, X. Zhang, F. Chen and Q. Fu, Aramid nanofiber framework supporting graphene nanoplate via wet spinning for a high-performance filament, *Carbon*, 2021, **179**, 655–665.
- 70 Z. Xu and C. Gao, Graphene chiral liquid crystals and macroscopic assembled fibers, *Nat. Commun.*, 2011, **2**, 571.
- 71 F. Liu, Q. Wang, G. Zhai, H. Xiang, J. Zhou, C. Jia, L. Zhu, Q. Wu and M. Zhu, Continuously processing waste lignin into high-value carbon nanotube fibers, *Nat. Commun.*, 2022, **13**, 5755.
- 72 J. Zhang, S. Seyedin, S. Qin, P. A. Lynch, Z. Wang, W. Yang, X. Wang and J. M. Razal, Fast and scalable wet-spinning of highly conductive PEDOT:PSS fibers enables versatile applications, *J. Mater. Chem. A*, 2019, **7**, 6401–6410.
- 73 L. Zheng, M. Zhu, B. Wu, Z. Li, S. Sun and P. Wu, Conductance-stable liquid metal sheath-core microfibers for stretchy smart fabrics and self-powered sensing, *Sci. Adv.*, 2021, **7**, eabg4041.
- 74 J. Wu, M. Wang, L. Dong, J. Shi, M. Ohyama, Y. Kohsaka, C. Zhu and H. Morikawa, A Trimode Thermoregulatory Flexible Fibrous Membrane Designed with Hierarchical Core-Sheath Fiber Structure for Wearable Personal Thermal Management, *ACS Nano*, 2022, **16**, 12801–12812.
- 75 J. Cao, F. Liang, H. Li, X. Li, Y. Fan, C. Hu, J. Yu, J. Xu, Y. Yin, F. Li, D. Xu, H. Feng, H. Yang, Y. Liu, X. Chen, G. Zhu and R.-W. Li, Ultra-robust stretchable electrode for e-skin: In situ assembly using a nanofiber scaffold and liquid metal to mimic water-to-net interaction, *InfoMat*, 2022, **4**, e12302.
- 76 P. Deng, Y. Wang, R. Yang, Z. He, Y. Tan, Z. Chen, J. Liu and T. Li, Self-Powered Smart Textile Based on Dynamic Schottky Diode for Human-Machine Interactions, *Adv. Sci.*, 2023, **10**, 2207298.
- 77 X. Shi, Y. Zuo, P. Zhai, J. Shen, Y. Yang, Z. Gao, M. Liao, J. Wu, J. Wang, X. Xu, Q. Tong, B. Zhang, B. Wang, X. Sun, L. Zhang, Q. Pei, D. Jin, P. Chen and H. Peng, Large-area display textiles integrated with functional systems, *Nature*, 2021, **591**, 240–245.
- 78 A. Levitt, D. Hegh, P. Phillips, S. Uzun, M. Anayee, J. M. Razal, Y. Gogotsi and G. Dion, 3D knitted energy storage textiles using MXene-coated yarns, *Mater. Today*, 2020, **34**, 17–29.
- 79 G. Shao, R. Yu, X. Zhang, X. Chen, F. He, X. Zhao, N. Chen, M. Ye and X. Y. Liu, Making Stretchable Hybrid Supercapacitors by Knitting Non-Stretchable Metal Fibers, *Adv. Funct. Mater.*, 2020, **30**, 2003153.
- 80 D. Du, P. Li and J. Ouyang, Graphene coated nonwoven fabrics as wearable sensors, *J. Mater. Chem. C*, 2016, **4**, 3224–3230.
- 81 F. Wang, J. Jiang, F. Sun, L. Sun, T. Wang, Y. Liu and M. Li, Flexible wearable graphene/alginate composite nonwoven fabric temperature sensor with high sensitivity and anti-interference, *Cellulose*, 2020, **27**, 2369–2380.
- 82 W. Zhang, J. Miao, M. Tian, X. Zhang, T. Fan and L. Qu, Hierarchically interlocked helical conductive yarn enables ultra-stretchable electronics and smart fabrics, *Chem. Eng. J.*, 2023, **462**, 142279.
- 83 T. Yan, G. Zhang, K. Yu, K. Yu, H. Chai, M. Tian, L. Qu, H. Dong and X. Zhang, Smartphone light-driven zinc porphyrinic MOF nanosheets-based enzyme-free wearable photoelectrochemical sensor for continuous sweat vitamin C detection, *Chem. Eng. J.*, 2023, **455**, 140779.
- 84 R. Xu, M. She, J. Liu, S. Zhao, H. Liu, L. Qu and M. Tian, Breathable Kirigami-Shaped Ionotronic e-Textile with Touch/Strain Sensing for Friendly Epidermal Electronics, *Adv. Fiber Mater.*, 2022, **4**, 1525–1534.
- 85 X. Liu, J. Miao, Q. Fan, W. Zhang, X. Zuo, M. Tian, S. Zhu, X. Zhang and L. Qu, Recent Progress on Smart Fiber and Textile Based Wearable Strain Sensors: Materials, Fabrications and Applications, *Adv. Fiber Mater.*, 2022, **4**, 361–389.
- 86 H. Park, J. W. Kim, S. Y. Hong, G. Lee, H. Lee, C. Song, K. Keum, Y. R. Jeong, S. W. Jin, D. S. Kim and J. S. Ha, Dynamically Stretchable Supercapacitor for Powering an Integrated Biosensor in an All-in-One Textile System, *ACS Nano*, 2019, **13**, 10469–10480.
- 87 G. Chen, H. Wang, R. Guo, M. Duan, Y. Zhang and J. Liu, Superelastic EGaIn Composite Fibers Sustaining 500% Tensile Strain with Superior Electrical Conductivity for Wearable Electronics, *ACS Appl. Mater. Interfaces*, 2020, **12**, 6112–6118.

- 88 Y. Ma, J. Ouyang, T. Raza, P. Li, A. Jian, Z. Li, H. Liu, M. Chen, X. Zhang, L. Qu, M. Tian and G. Tao, Flexible all-textile dual tactile-tension sensors for monitoring athletic motion during taekwondo, *Nano Energy*, 2021, **85**, 105941.
- 89 Z. Li, S. Zhang, Y. Chen, H. Ling, L. Zhao, G. Luo, X. Wang, M. C. Hartel, H. Liu, Y. Xue, R. Haghniaz, K. Lee and W. Sun, Gelatin Methacryloyl-Based Tactile Sensors for Medical Wearables, *Adv. Funct. Mater.*, 2020, **30**, 2003601.
- 90 H. Kim, A. Shaqeel, S. Han, J. Kang, J. Yun, M. Lee, S. Lee, J. Kim, S. Noh, M. Choi and J. Lee, In Situ Formation of Ag Nanoparticles for Fiber Strain Sensors: Toward Textile-Based Wearable Applications, *ACS Appl. Mater. Interfaces*, 2021, **13**, 39868–39879.
- 91 J. Miao, M. Tian, L. Qu and X. Zhang, Flexible, transparent and conductive wearable electronic skin based on 2D titanium carbide (MXene) ink, *Carbon*, 2024, **222**, 118950.
- 92 P. Zhao, Y. Song, Z. Hu, Z. Zhong, Y. Li, K. Zhou, T. Qin, Y. Yan, H.-H. Hsu, S.-T. Han, V. A. L. Roy, C. C. Kuo and Y. Zhou, Artificial intelligence enabled biodegradable all-textile sensor for smart monitoring and recognition, *Nano Energy*, 2024, **130**, 110118.
- 93 H. Lu, Y. Zhang, M. Zhu, S. Li, H. Liang, P. Bi, S. Wang, H. Wang, L. Gan, X.-E. Wu and Y. Zhang, Intelligent perceptual textiles based on ionic-conductive and strong silk fibers, *Nat. Commun.*, 2024, **15**, 3289.
- 94 K. Li, T.-H. Chang, Z. Li, H. Yang, F. Fu, T. Li, J. S. Ho and P.-Y. Chen, Biomimetic MXene Textures with Enhanced Light-to-Heat Conversion for Solar Steam Generation and Wearable Thermal Management, *Adv. Energy Mater.*, 2019, **9**, 1901687.
- 95 X. Liang, H. Li, J. Dou, Q. Wang, W. He, C. Wang, D. Li, J.-M. Kin and Y. Zhang, Stable and Biocompatible Carbon Nanotube Ink Mediated by Silk Protein for Printed Electronics, *Adv. Mater.*, 2020, **32**, 2000165.
- 96 Y. Jing, M. Du, P. Zhang, Z. Liang, Y. Du, L. Yao, H. Chen, T. Zhang and K. Zhang, Advanced cooling textile technologies for personal thermoregulation, *Mater. Today Phys.*, 2024, **41**, 101334.
- 97 Y. Ni, D. Yang, T. Hu, Q. Wei, W. Guo and L. Zhang, Fabrication of natural rubber dielectric elastomers with enhanced thermal conductivity via dopamine chemistry, *Compos. Commun.*, 2019, **16**, 132–135.
- 98 S. Mateti, K. Yang, X. Liu, S. Huang, J. Wang, L. H. Li, P. Hodgson, M. Zhou, J. He and Y. Chen, Bulk Hexagonal Boron Nitride with a Quasi-Isotropic Thermal Conductivity, *Adv. Funct. Mater.*, 2018, **28**, 1707556.
- 99 T. Gao, Z. Yang, C. Chen, Y. Li, K. Fu, J. Dai, E. M. Hitz, H. Xie, B. Liu, J. Song, B. Yang and L. Hu, Three-Dimensional Printed Thermal Regulation Textiles, *ACS Nano*, 2017, **11**, 11513–11520.
- 100 Y. Song, F. Jiang, N. Song, L. Shi and P. Ding, Multilayered structural design of flexible films for smart thermal management, *Composites, Part A*, 2021, **141**, 106222.
- 101 X.-E. Wu, Y. Wang, X. Liang, Y. Zhang, P. Bi, M. Zhang, S. Li, H. Liang, S. Wang, H. Wang, H. Lu and Y. Zhang, Durable Radiative Cooling Multilayer Silk Textile with Excellent Comprehensive Performance, *Adv. Funct. Mater.*, 2024, **34**, 2313539.
- 102 Y. Wang, Z. Wang, H. Huang, Y. Li and W. Zhai, A Camel-Fur-Inspired Micro-Extrusion Foaming Porous Elastic Fiber for All-Weather Dual-Mode Human Thermal Regulation, *Adv. Sci.*, 2024, **11**, e2407260.
- 103 R. Wu, C. Sui, T.-H. Chen, Z. Zhou, Q. Li, G. Yan, Y. Han, J. Liang, P.-J. Hung and P.-C. Hsu, Spectrally engineered textile for radiative cooling against urban heat islands, *Science*, 2024, **384**, 1203–1212.
- 104 Z. Li, Y. Yuan, L. Wu, L. Qin, M. Zhou, Y. Yu, Q. Wang and P. Wang, Hierarchically Engineered Silk Fibroin Nanotextiles with Spectral Selectivity and Asymmetric Nanostructure for Sustainable Personal Thermal-Wet Regulation, *Adv. Fiber Mater.*, 2025, **7**, 1475–1494.
- 105 B. Yan, M. Zhou, X. Liao, P. Wang, Y. Yu, J. Yuan and Q. Wang, Developing a Multifunctional Silk Fabric with Dual-Driven Heating and Rapid Photothermal Antibacterial Abilities Using High-Yield MXene Dispersions, *ACS Appl. Mater. Interfaces*, 2021, **13**, 43414–43425.
- 106 J. Wu, M. Zhang, M. Su, Y. Zhang, J. Liang, S. Zeng, B. Chen, L. Cui, C. Hou and G. Tao, Robust and Flexible Multimaterial Aerogel Fabric Toward Outdoor Passive Heating, *Adv. Fiber Mater.*, 2022, **4**, 1545–1555.
- 107 N. Cheng, Z. Wang, Y. Lin, X. Li, C. Ding, C. Wang, J. Tan, F. Sun, X. Wang, J. Yu and B. Ding, Breathable Dual-Mode Leather-Like Nanotextile for Efficient Daytime Radiative Cooling and Heating, *Adv. Mater.*, 2024, **36**, 2403223.
- 108 Z. Luo, B. Li, H. Sun, J. Liu, H.-Y. Zhao and D. Yang, Dual-functional reduced graphene oxide decorated nanoporous polytetrafluoroethylene metafabrics for radiative cooling and solar-heating, *J. Mater. Chem. A*, 2023, **11**, 16595–16604.
- 109 B.-Y. Liu, J. Wu, C.-H. Xue, Y. Zeng, J. Liang, S. Zhang, M. Liu, C.-Q. Ma, Z. Wang and G. Tao, Bioinspired Superhydrophobic All-In-One Coating for Adaptive Thermoregulation, *Adv. Mater.*, 2024, **36**, 2400745.
- 110 C. Yang, C. Chen, D. Tao, K. Yan, H. You, Q. Liu, W. Wang and D. Wang, Facile design of nanofiber composite film with multi-level crosslinked enhanced structure using carbon nanotubes/silver-coated nylon 6 as microwave absorber, *Chem. Eng. J.*, 2025, **507**, 160188.
- 111 Y. Niu, Z. Wang, Y. Li, B. Huang, T. Ma, X. Jiang, H. Cheng, K. Zhang and C. Yi, Ultrathin MXene/Ag-Ag nanocomposite films for 3D-conformable electromagnetic shielding via aerosol jet printing, *Chem. Eng. J.*, 2025, **506**, 160112.
- 112 A. Liu, X. Qiu, X. Lu, H. Guo, J. Hu, C. Liang, M. He, Z. Yu, Y. Zhang, J. Kong and J. Gu, Asymmetric structural MXene/PBO Aerogels for High Performance Electromagnetic Interference shielding with Ultra-Low Reflection, *Adv. Mater.*, 2025, **37**, 2414085.
- 113 C. Gao, T. Liu, B. Luo, C. Cai, W. Zhang, J. Zhao, J. Yuan, P. Fatehi, C. Qin and S. Nie, Cellulosic tri-

- boelectric materials for stable energy harvesting from hot and humid conditions, *Nano Energy*, 2023, **111**, 108426.
- 114 Y. Li, Y. Zhang, J. Yi, X. Peng, R. Cheng, C. Ning, F. Sheng, S. Wang, K. Dong and Z. L. Wang, Large-scale fabrication of core-shell triboelectric braided fibers and power textiles for energy harvesting and plantar pressure monitoring, *EcoMat*, 2022, **4**, e12191.
- 115 J. He, C. Lu, H. Jiang, F. Han, X. Shi, J. Wu, L. Wang, T. Chen, J. Wang, Y. Zhang, H. Yang, G. Zhang, X. Sun, B. Wang, P. Chen, Y. Wang, Y. Xia and H. Peng, Scalable production of high-performing woven lithium-ion fiber batteries, *Nature*, 2021, **597**, 57–63.
- 116 J. Chen, Y. Huang, N. Zhang, H. Zuo, R. Liu, C. Tao, X. Fan and Z. L. Wang, Micro-cable structured textile for simultaneously harvesting solar and mechanical energy, *Nat. Energy*, 2016, **1**, 16138.
- 117 Z. Wen, M.-H. Yeh, H. Guo, J. Wang, Y. Zi, W. Xu, J. Deng, L. Zhu, X. Wang and Z. L. Wang, Self-powered textile for wearable electronics by hybridizing fiber-shaped nanogenerators, solar cells, and supercapacitors, *Sci. Adv.*, 2016, **2**, e1600097.
- 118 Z. Hou, X. Liu, M. Tian, X. Zhang, L. Qu, T. Fan and J. Miao, Smart fibers and textiles for emerging clothe-based wearable electronics: materials, fabrications and applications, *J. Mater. Chem. A*, 2023, **11**, 17336.
- 119 A. Shi, B. Luo, W. Chen, Z. Li, S. Wang, L. Jiang, H. Zhang, X. Qin and W. Sun, A Facile Strategy for Textile-Based Highly Sensitive and Water Resistant Triboelectric Nanogenerator, *Adv. Mater.*, 2025, **37**, 2420459.